
Electronic Thesis and Dissertation Repository

9-29-2017 2:00 PM

An Investigation of the CK2-dependent Phosphoproteome using Inhibitor Refractory CK2-alpha

Edward Cruise, *The University of Western Ontario*

Supervisor: David W Litchfield, *The University of Western Ontario*

A thesis submitted in partial fulfillment of the requirements for the Master of Science degree in Biochemistry

© Edward Cruise 2017

Follow this and additional works at: <https://ir.lib.uwo.ca/etd>

 Part of the [Biochemistry Commons](#), and the [Molecular Biology Commons](#)

Recommended Citation

Cruise, Edward, "An Investigation of the CK2-dependent Phosphoproteome using Inhibitor Refractory CK2-alpha" (2017). *Electronic Thesis and Dissertation Repository*. 5164.
<https://ir.lib.uwo.ca/etd/5164>

This Dissertation/Thesis is brought to you for free and open access by Scholarship@Western. It has been accepted for inclusion in Electronic Thesis and Dissertation Repository by an authorized administrator of Scholarship@Western. For more information, please contact wlsadmin@uwo.ca.

Abstract

Protein kinase CK2 is a constitutively active serine/threonine kinase that is overexpressed in several human cancers, and by virtue of the vast number of putative substrates in the phosphoproteome, is implicated in the regulation of numerous cellular processes. Consequently, CK2 is an emerging therapeutic target with many CK2 inhibitors having been developed. An example of one such inhibitor is the clinical stage compound CX-4945. Although highly selective for CK2, the ATP competitive CX-4945 has demonstrated affinity for other kinases. Unique features of the catalytic pocket of CK2 have allowed for the development of inhibitor refractory mutants, which have since been stably integrated into tetracycline inducible osteosarcoma cell lines. A mass spectrometry-based phosphoproteomic workflow was used in conjunction with inhibitor refractory cell lines to study the impact of CK2 inhibition on the phosphoproteome, and potentially identify off-targets of the clinical compound CX-4945. In response to CX-4945 treatment the inhibitor refractory mutant recovered phosphorylation at several sites, revealing potential novel substrates of CK2. Phosphoproteomic analysis also revealed potential off-targets of CX-4945. This investigation provides valuable insight into the role played by CK2 in cellular signaling and provides a platform for downstream targeted proteomic analysis of CK2.

Keywords:

CK2, Proteomics, Phosphorylation, CX-4945, Kinase, Inhibitor, Mass Spectrometry, Phosphoproteome

Co-Authorship Statement

All sections in this thesis were written by Edward Cruise and edited by David Litchfield. Edward Cruise performed all of the experiments and data analysis with the exception of Supplementary Figure 5 which was performed by Stephanie Zuckowski. Paul Desormeaux also helped with a number of the inhibitor time-course experiments. Kristina Jurcic ran the samples for mass spectrometry experiments

Acknowledgments

First, I would like to thank Dave Litchfield for taking me on as a graduate student in his laboratory. It was a privilege to have spent the past three years under his supervision. Since the beginning he has been a source of valuable insight and provided me with an environment where my interests could be pursued without any obstacles.

A special thanks is required for Dr. Laszlo Gyenis. He played a significant role in my training as a biochemist. I could not have asked for a better mentor, and consider myself extremely lucky to be one of the many student researchers to have passed under his tutelage. Thank you to all the members of the Litchfield lab past and present: Sam Fess, Stephanie Zuckowski, Teresa Nuñez de Villavicencio Diaz, Viviana Hermosilla-Aguayo, Michelle Gabriel, Michelle Dubinsky, Shahbaz Khan, Paul Desormeaux, Jurgen Vahter, Adam Rabalski, Kristina Jurcic, Tim Leung, James Plaetzer, and Kevin Krysiak. Whether it was scientific discussion or friendly banter over pints at the grad club, I always enjoyed your company. I will look back fondly on the time I spent with you all. I'd also like to thank the members of my advisory committee, Murray Junop, Gabe DiMattia, and Gilles Lajoie for their advice and feedback.

I'd like to thank my parents for their constant support. You instilled in me a natural curiosity and drive that led me to research. I am very fortunate to have parents who engaged me in science at an early age. I would also like to thank my girlfriend Melissa, whose presence has always helped me escape from the stresses of life no matter their severity.

Table of Contents

Co-Authorship Statement.....	ii
Acknowledgments.....	iii
Table of Contents	iv
List of Tables	vi
List of Figures	vii
List of Abbreviations	ix
1 Chapter 1 - Introduction	1
1.1 General Introduction	1
1.2 Protein Kinase CK2	2
1.3 Role of CK2 in Pro-Survival Pathways	3
1.4 CK2 in Cancer.....	4
1.5 Pharmacological Inhibition of CK2	6
1.6 CX-4945: A Highly Selective and Potent ATP-competitive CK2 Inhibitor.....	7
1.7 Tools for Validating Inhibitor Selectivity and CK2 Dependent Signaling.....	11
1.8 Deciphering CX-4945 Off-Targets: Inhibitor Refractory CK2 Mutants	12
1.9 Mass Spectrometry Based Proteomics.....	12
1.10Quantitative Proteomics.....	14
1.11Phosphoproteomics	16
1.12Thesis Objective and Rationale	17
2 Experimental Methods	21
2.1 Cell Culture, Lysis & Western Blotting for Sustained Induction Experiments	21
2.2 Preliminary Inhibitor Time-courses	22

2.3	Immunoprecipitation.....	22
2.4	SILAC Medium Formulation.....	23
2.5	SILAC Incorporation of Flp-U2OS Cells.....	24
2.6	CX-4945 Treatment and Lysis of SILAC Flp-U2OS Cells.....	25
2.7	LC-MS/MS Data Acquisition.....	26
2.8	Sample Digestion and Phosphopeptide Enrichment.....	29
2.9	Data Analysis.....	31
3	Results.....	32
3.1	Characterization of U2OS Cell Lines Expressing Wild-type and Inhibitor-Refractory Mutants of CK2-alpha.....	32
3.2	Investigating the CK2 Dependent Phosphoproteome.....	39
3.3	Inhibitor Refractory CK2-alpha Restores Phosphorylation in the Presence of CX-4945.....	42
3.4	Dynamic Changes in the Phosphoproteome are Independent of Protein Abundance.....	48
3.5	CX-4945 Treatment Modulates the Activity of Other Kinases.....	50
4	Discussion.....	55
5	Supplemental Figures.....	69
	Bibliography.....	80
	Curriculum Vitae.....	90

List of Tables

Table 1. Phosphosites inhibited following CX-4945 treatment restored by inhibitor-refractory CK2-alpha.	53
--	----

List of Figures

Figure 1. Crystal Structure of CX-4945 in Complex with CK2-alpha Catalytic Subunit (PDB: 3PE1).....	9
Figure 2. Chemical structures of ATP, GTP and CK2 inhibitor CX-4945.....	10
Figure 3. Sustained Exogenous Expression of Wild-type and Inhibitor Refractory CK2-alpha.	34
Figure 4. Exogenous CK2-alpha forms complexes with endogenous CK2 β	36
Figure 5. Preliminary Time-Course Treatment of Engineered Flp-U2OS cells with 30 μ M CX-4945.....	38
Figure 6. Workflow to Investigate CK2 dependent Phosphoproteome.	44
Figure 7. Experimental Layout and Data Summary	45
Figure 8. Volcano Plot of Quantified Phosphorylation sites from Inhibitor-Resistant U2OS cells treated with CX-4945.	46
Figure 9. Analysis of Recovered Phosphorylation Sites.....	47
Figure 10. Comparison of Phosphorylation Site vs. Protein Abundance in Inhibitor Resistant U2OS cells treated with CX-4945.	49
Figure 11. Kinase Perturbation Analysis Reveals Off-Targets of CX-4945.	52
Supplemental Figure 1. Measuring the ability of CK2-alpha mutants to overcome the inhibition of CX-4945.....	69
Supplemental Figure 2. Optimal CX-4945 concentration for the inhibition of CK2 in U2OS cells expressing wild-type and inhibitor refractory (V66A/I174A/H160D) CK2-alpha.	70
Supplemental Figure 3. Frequency Distribution of SILAC Medium Labelled Arginine and Lysine Incorporated Peptides.....	71
Supplemental Figure 4. Frequency Distribution of Heavy Labelled SILAC Arginine and Lysine Incorporated Peptides.....	72
Supplemental Figure 5. Preliminary Time-Course treatment of U2OS cells with 50 μ M CX-4945 and 1 μ M Staurosporine.....	73
Supplemental Figure 6. Quantified CK2 Phosphorylation Sites in PhosphositePlus in U2OS Cells Treated with 30 μ M CX-4945..	74

Supplemental figure 7. Frequency Distribution of Protein Mean Log2 Ratio in Flp-U2OS cells expressing wild-type CK2-alpha treated with 30 μ M CX-4945 for 4 hours.....	75
Supplemental Figure 8. Frequency Distribution of Protein Mean Log2 Ratio in Flp-U2OS cells expressing inhibitor-refractory CK2-alpha treated with 30 μ M CX-4945 for 4 hours. .	76
Supplemental Figure 9. Frequency Distribution of Phosphorylation Site Mean Log2 Ratio in Flp-U2OS cells expressing inhibitor-refractory CK2-alpha treated with 30 μ M CX-4945 for 4 hours.....	77
Supplementary Figure 10. Frequency Distribution of Phosphorylation Site Mean Log2 Ratio in Flp-U2OS cells expressing With-Type CK2-alpha treated with 30 μ M CX-4945 for 4 hours.....	78
Supplemental Figure 11. Bi-plot of Phosphorylation Site Mean Log2 Fold Changes for U2OS Cells Expressing either Wild-Type or Inhibitor Refractory CK2-alpha Treated with 30 μ M CX-4945.....	79

List of Abbreviations

°C	degrees centigrade
7-AAD	7-amino-actinomycin D
Å	angstrom
ABC	ammonium bicarbonate
ACN	acetonitrile
ATP	adenosine triphosphate
BSA	bovine serum albumin
CDK	cyclin dependent kinase
CID	collision induced dissociation
CK2	protein kinase CK2
CK2 α	catalytic isoform of CK2 alpha, CSNK2A1
CK2 α'	catalytic isoform of CK2 alpha prime, CSNK2A2
CK2 β	catalytic isoform of CK2 beta, CSNK2B
CML	chronic myelogenous leukemia
CX-4945	5-((3-chlorophenyl)amino)benzo[c][2,6]naphthyridine-8-carboxylic acid
Da	Dalton
DMEM	Dulbecco's modified Eagle medium
DMSO	dimethyl sulfoxide
DTT	D-Dithiothreitol
EDTA	ethylenediaminetetraacetic acid
EIF2S2	eukaryotic translation initiation factor 2 subunit 2
eIF2B	eukaryotic translation initiation factor 2 subunit 2

ERK	extracellular signal-regulated kinase
FA	formic acid
FBS	fetal bovine serum
FDR	false discovery rate
g	relative centrifugal force
GAM	goat-anti-mouse
GAPDH	glyceraldehyde 3-phosphate dehydrogenase
GAR	goat-anti-rabbit
GdmCl	Guanidium Chloride
HeLa	human cervical cancer cell line
HPLC	high performance liquid chromatography
IAA	iodoacetamide
Inhibitor VIII	4-(2-(4-methoxybenzamido)thiazol-5-yl)benzoic acid
IR	Inhibitor Refractory
KCl	potassium chloride
kDa	kiloDalton
L	liter
LC	liquid chromatography
Lys-C	endoproteinase Lys-C
m/z	mass-to-charge ratio
MAPK	mitogen activated protein kinase
MEK	MAPK/ERK kinase
mg	milligram
mL	millilitre

mM	millimolar
MS	mass spectrometer
MS1	survey scan of mass spectrometer cycle
MS2	dependent scan of mass spectrometer cycle
mTOR	mechanistic or mammalian target of rapamycin
NCE	normalized collision energy
NCS	neocarzinostatin
nm	nanometre
NP-40	Nonidet P-40
p70S6K	ribosomal protein S6 kinase beta-1, RPS6KB1
PARP-1	poly (ADP-ribose) polymerase
PBS	phosphate buffered saline
PBST	phosphate buffered saline + 0.1% Tween-20
PMSF	phenylmethylsulfonylfluoride
ppm	parts per million
PRM	parallel reaction monitoring
PVDF	polyvinylidene fluoride
SCX	strong cation exchange chromatography
SDS	sodium dodecyl sulfate
SDS-PAGE	sodium dodecyl sulfate – polyacrylamide gel electrophoresis
SILAC	Stable Isotope Labeling of Amino Acids in Cell Culture
STS	staurosporine
TBST	Tris buffered saline + 0.05% Tween-20
TOP2A	topoisomerase 2 alpha

TRAIL	Tumor necrosis factor-related apoptosis-inducing ligand
Tris	tris(hydroxymethyl)aminomethane
TM	Triple Mutant
U2OS	Human Osteosarcoma Cells
μg	microgram
μL	microlitre
μm	micrometre
μM	micromolar

1 Chapter 1 - Introduction

1.1 General Introduction

The phosphorylation of proteins mediated by protein kinases is a critical element in the orchestration of cellular signaling pathways (1). Via the transfer of phosphate from the terminal phosphate of ATP to the hydroxyl groups of serine, threonine, and tyrosine residues, kinases regulate essential processes such as gene expression, protein structure and binding and cellular responses to external stimuli (2). The elucidation of the human genome has allowed for the identification of 518 protein kinases, having the combined potential to phosphorylate over 700 000 serine, threonine and tyrosine residues in the human proteome (3). Given the fundamental nature of the processes they control, the necessity for kinases to carry out their intended functions is self-evident. Perturbations in kinase mediated signaling pathways can have dramatic effects on cell growth, proliferation and apoptosis which can manifest themselves in a variety of diseases including cancer (4). Therefore, the involvement of kinases in such pathological processes has prompted their interest as targets for therapeutics (5). The development and success of Gleevec (Imatinib), a protein kinase inhibitor targeting the Bcr-Abl fusion protein for the treatment of chronic myelogenous leukemia, provides validation for the targeting of protein kinases as therapeutics and serves as a proof of principle for the knowledge based design of protein kinase inhibitors (6). Kinases now represent the largest category of drug targets with clinical potential (7). According to the FDA, 145

unique kinases have been identified as targets of established clinical trial compounds, with 93 of these representing novel targets for which FDA approved pharmaceuticals have not yet been directed. Within the categories of protein kinases, serine/threonine kinases have seen the largest growth as therapeutic targets (7).

1.2 Protein Kinase CK2

Protein kinase CK2 (casein kinase II) is a constitutively active, messenger independent serine/threonine kinase that is ubiquitously expressed and essential for viability in eukaryotes (8, 9). CK2 is composed of two closely related catalytic isoforms designated alpha (CSNK2A1) and alpha' (CSNK2A2). These subunits are the products of different genes, and have over 90% sequence homology apart from their c-terminal domains (10). Each catalytic subunit can function independently, or in the holo-enzyme form in which two of either CK2alpha or CK2alpha' are complexed with two regulatory CK2beta (CSNK2B) subunits (11). In this respect, CK2 is distinct from cyclin dependent kinases, whose activity is dependent upon the presence of an activating cyclin and from an activating phosphorylation event by an upstream kinase. As mentioned, CK2beta is not required for catalytic activity, however, it has been found to play a role in substrate recognition as well as providing a protective and stabilizing role (12). Although there are no known differences in the activity of its catalytic subunits, there is evidence that CK2alpha and CK2alpha' exhibit functional specialization. For example, caspase-3 has been shown to be preferentially phosphorylated by CK2alpha' rather than CK2alpha despite their similarities (13). Both catalytic subunits recognize a consensus sequence of serine/threonine residues N-terminal to clusters of acidic residues, with a minimal

consensus requirement of S/T-X-X-D/E (14). Analysis of CK2 in the literature, as well as computational predictions based on its consensus sequence, suggest CK2 has the potential to phosphorylate over 2000 sites in the human proteome (15). CK2 is a very highly conserved enzyme, and is implicated in many essential cellular signaling processes including transcription, translation, circadian rhythms, cell cycle progression and cell survival (16–19). Dysregulation of any one of these pathways has the potential to result in disease states, including cancer. Given the overlap between the pathways in which CK2 is known to play a central role and the pathways that make up the hallmarks of cancer, it comes as no surprise that alterations in CK2 activity could result in cancer.

1.3 Role of CK2 in Pro-Survival Pathways

With respect to the potential role of CK2 to promote a cancerous phenotype, an anti-apoptotic role has been suggested given several intriguing observations. Interestingly, the minimal consensus sequence required for phosphorylation by CK2 and that required for cleavage by caspases have striking overlap (20, 21). Given the proximity of CK2 phosphorylation sites to caspase cleavage sites, it has been suggested that upregulated CK2 phosphorylation may act as a mechanism to impede caspase cleavage and thereby impede the progression of apoptosis and promote cell survival (22). In fact, there are a number of documented cases in which caspase substrates such as Bid and YY1, which promote the progression of apoptosis when cleaved, can be phosphorylated by CK2 adjacent to those cleavage sites (23, 24). Biochemical and computational approaches were employed to build on these observations and subsequently revealed several caspase substrates whose cleavage sites overlapped with sites conforming to the

CK2 consensus sequence for phosphorylation (25, 26). These observations suggest CK2 could have a widespread role in regulating the activity of caspases by impeding their ability to cleave their targets. In addition to the observation that CK2 and caspase substrates overlap, it was found that CK2 is implicated in mediating the activity of caspases themselves. The screen also revealed that phosphorylation of caspase-3 by CK2 prevents its cleavage and thus its activation by upstream caspases (13). Taken together these findings suggest a mechanism whereby the constitutive activity of CK2 enables it to promote a “pathological rewiring” of caspase pathways through elevated levels of phosphorylation of caspase substrates. Therefore, the expression of CK2 at abnormally high levels such as those found in cancers could lead to enhanced cell survival by evading apoptosis.

1.4 CK2 in Cancer

Early evidence for the involvement of CK2 in malignancies was shown in breast and colorectal cancers, where its activity was up to 8-fold greater than its activity in cells of healthy individuals (27). Elevated activity of CK2 has since been observed in several cancers including cancers of the head and neck, kidney, mammary gland, and prostate among others (28–31). A direct association between CK2 and cancer was demonstrated in transgenic mouse models, where targeted overexpression of CK2 in T-cells and mammary gland epithelium lead to lymphomagenesis and mammary tumorigenesis (32, 33). Although a precise role for CK2’s contributions to an oncogenic phenotype remain unclear, its importance in maintaining such phenotypes has become increasingly evident simply by virtue of its vast network of substrates and interacting partners categorized as

tumour suppressors, oncogenes, and pro-apoptotic proteins. In most cases, elevated CK2 activity is neither cause nor consequence of neoplastic transformation. Rather, it could be seen as a reflection of a tumours tendency to preferentially colonize cells where CK2 activity is elevated (34, 35). CK2 is unique, in that it is characterized as an agent that promotes both intrinsic and extrinsic oncogenic processes as a consequence of its involvement in a considerable number of pathways. Extrinsic processes (i.e.: those that occur outside of the plasma membrane) in which CK2 can promote cancer include its role in angiogenesis through the HIF-1 α pathway, which serves to promote the tumour microenvironment (36). Intrinsically, elevated CK2 activity can promote the tumour phenotype in several key ways. Apart from its ability to enhance the transformation potential of oncogenes, CK2 stabilizes the onco-kinome through the phosphorylation of Hsp90 co-chaperone cdc37 on serine 13, which serves to maintain kinases in their active conformations (37, 38). Additionally, CK2 contributes to the multi-drug resistant phenotype. Demonstrated inhibition of CK2 has been shown to result in the increased uptake of pharmacological agents, presumably due to the phosphorylation of the P-glycoprotein transporter (39).

Typically, these findings involve CK2 α overexpression. However, there are reported instances where dysregulation of CK2 α and CK2 β have been implicated in cancer. Analysis of the Oncomine database revealed deregulation of both CK2 α and CK2 β (40, 41), as well as the CK2 α pseudogene transcript expression in neoplastic tissue when compared to normal tissue (42). CK2 is not a prototypical “oncogene”, in the sense that there are no instances of genetic alterations in CK2 leading to its uncontrolled activity and subsequent tumorigenesis. Dysregulated oncogenes serve

as the causative agents in cancer since their dysregulation forms the foundation for uncontrolled cellular proliferation. Instead, reliance of the tumour phenotype on CK2 activity is an example of “non-oncogene” addiction. Mechanistically, elevated CK2 activity provides a favorable cellular environment for perturbations in oncogenes to manifest themselves as cancer (34).

1.5 Pharmacological Inhibition of CK2

CK2’s involvement in a number of essential cellular processes which have been highlighted, as well as its levels of deregulation in a number of cancers have made it an attractive target for the development of targeted therapeutics (40, 43). Indeed, there are now several small-molecule and peptide inhibitors which have been patented as CK2-specific (44, 45). Despite the increasing number of CK2 directed agents that have become available, few of them have been fully characterized using unbiased methods. Therefore, the interest in CK2 directed therapeutics prompted investigations into the selectivity of CK2 inhibitors. A combined chemical and functional proteomic approach was devised to assess the efficacy of these commercially available compounds. From this it was demonstrated that earlier inhibitors of CK2 previously thought of as “highly selective” displayed poor selectivity and targeted many proteins other than their intended target (46). Two compounds have since demonstrated superior ability to inhibit CK2 with relatively high selectivity, namely compounds CX-4945 and CK2 Inhibitor VIII. Inhibitor VIII was uncovered by Hou et al (2012) (105), who discovered the compound by employing structure-based virtual screening using X-ray crystallographic data. Subsequent in-vitro assays with the compound demonstrated high selectivity and potent

cytotoxicity, indicating it could be a promising compound for cancer treatment. A structure-activity-relationship study performed by Pierre et al (2011) revealed the compound CX-4945 (47), displaying much higher potency and selectivity compared to available compounds as well as clinical promise and has since been the inhibitor of choice when studying CK2. The following section will focus on the use and characteristics of CX-4945.

1.6 CX-4945: A Highly Selective and Potent ATP-competitive CK2 Inhibitor

CX-4945 (silmitasertib) was developed by Cyclene Pharmaceuticals. The unique structure of CK2's catalytic site compared to that of other kinases allow for ATP-competitive inhibitors to be designed with high specificity (48). CX-4945 was designed to take advantage of CK2's relatively tight binding pocket. CK2 possesses bulkier residues, namely Valine 66 and Isoleucine 174 in locations that are traditionally occupied by smaller residues in other kinases (Figure 1) (49). CX-4945 is a potent inhibitor of recombinant human CK2 (CK2a IC₅₀ = 1 nmol/L and K_i = 0.38 nmol/L ± 0.02; CK2a0 IC₅₀ = 1 nmol/L)(Figure 2) (50). When tested for selectivity against a panel of 238 kinases, representing close to half of the known kinome, CX-4945 showed minimal inhibitory activity outside of its intended target with only 7 other kinases were inhibited greater than 90% (50). Cell based assays demonstrated that CX-4945 was functionally inactive against these kinases. Profiling of CX-4945 against a diverse panel of cancer cell lines revealed broad antiproliferative activity (50). Treatment with CX-4945 resulted in the attenuation of PI3K/Akt signalling in BT-474 breast cancer cells and BxPC-3

pancreatic cancer cell lines as evident by decreased phosphorylation of S129 on Akt, accompanied with dephosphorylation of the canonical Akt regulatory sites T308/S473 (50). Interestingly, CX-4945 treatment also resulted in cell-cycle arrest in a cell type dependent manner. BP-474 cells were arrested in G2/M upon treatment, while BxPC-3 cells were arrested in G1(50). In addition, there was universal activation of caspase3/7 pathways after 24 hrs of treatment in all cell lines tested (50). CX-4945 also displayed potent anti-tumour activity in mouse xenograft models. Currently, Senshwa Biosciences is investigating CX-4945 in Phase I/II clinical trials (clinical trials identifier: NCT02128282) for the treatment of cholangiocarcinoma in combination with gemcitabine and cisplatin. The goal of this clinical study is to determine the maximum tolerable dose, and an objective response rate in solid tumors.

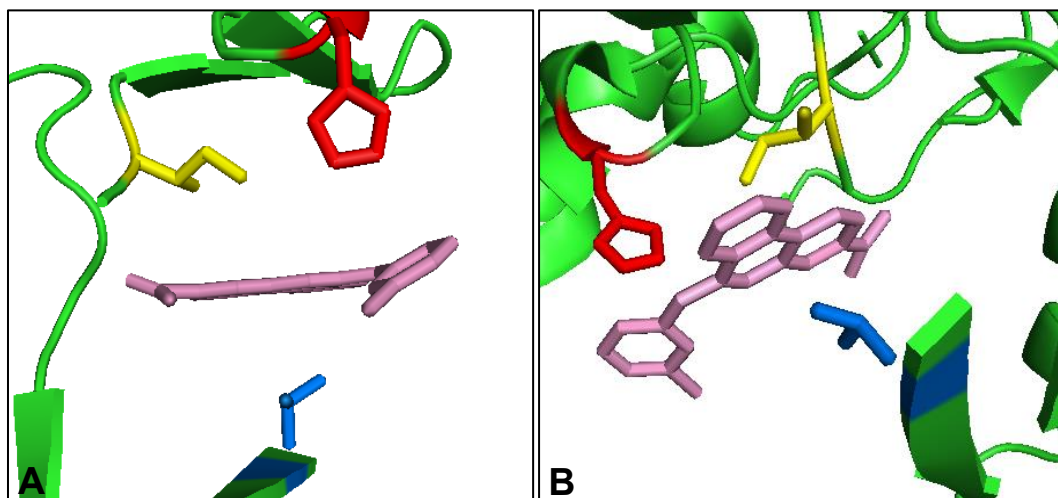


Figure 1. Crystal Structure of CX-4945 in Complex with CK2-alpha Catalytic Subunit (PDB: 3PE1). (A) Horizontal orientation of CX-4945 in complex with wild-type CK2-alpha catalytic subunit. CX-4945 (purple) is flanked by Histidine 160 (red), Isoleucine 174 (yellow), and Valine 66 (blue). The structure shown has been modified by the removal of some select residues not contributing to CX-4945 binding. (B) Orientation of CX-4945 demonstrating functional group location with respect to the highlighted amino acids.

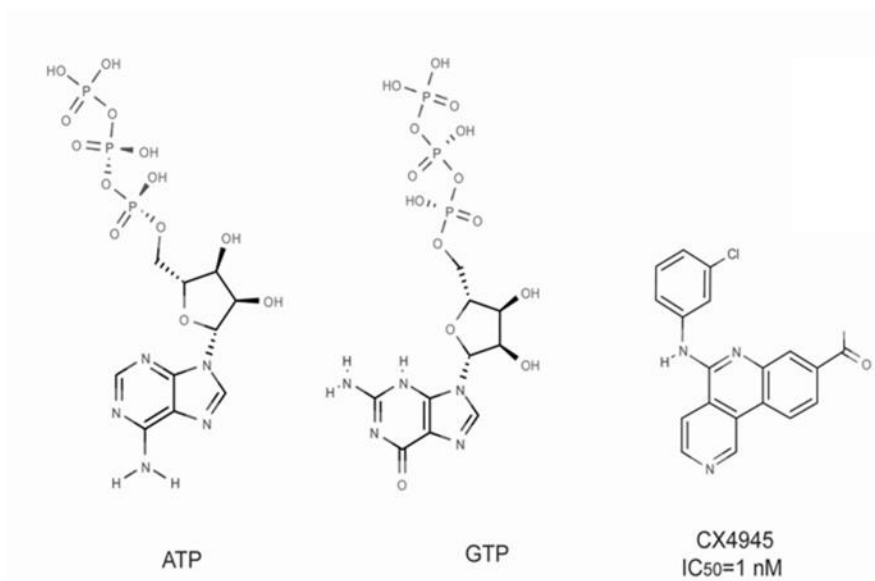


Figure 2. Chemical structures of ATP, GTP and CK2 inhibitor CX-4945.

Chemical structures of ATP, GTP, and characterized inhibitors, CX-4945 and Inhibitor VIII, of protein kinase CK2. Previously reported IC₅₀ values have also been included.

1.7 Tools for Validating Inhibitor Selectivity and CK2 Dependent Signaling

Although CX-4945 has demonstrated remarkable selectivity and potency towards CK2 in pre-clinical studies, the extent to which it binds other proteins has not been carefully examined. Most drug types suffer from the limitation of off-target binding, however, it is especially true of drugs targeting kinases due to their shared structural similarities. Given these limitations it is essential that strategies be developed to validate target engagement by the inhibitor. The importance of this is not only to justify their use as therapeutic agents, but to ensure the proper interpretation of biological experiments that rely on inhibitors to modulate the activity of a pathway. Obviously, any strategy that is developed to address these concerns must account for the individual nuances with respect to the kinase of interest. In the case of CK2, there are a few aspects of its functionality that must be considered when developing such strategies. First, the fact that CK2 is constitutively active and essential for viability generates a situation where the investigator must be conscious of toxicity resulting from CK2 inhibition. Second, because of the broad nature of CK2's involvement in biological processes, a mechanistic analysis of CK2 in a cellular context must be done on a global scale to obtain any meaningful information. With these considerations in mind we have developed strategies to systematically evaluate the effectiveness of CK2 inhibitors, while concurrently obtaining a mechanistic analysis of CK2's role in cellular processes. The following sections will outline the biochemical tools used for these investigations.

1.8 Deciphering CX-4945 Off-Targets: Inhibitor Refractory CK2 Mutants

To distinguish between the on and off-target effects of treatment with CX-4945, we have developed inhibitor refractory mutants of the CK2 α catalytic subunit. High resolution structures of CK2 in complex with CX-4945 revealed extensive interactions with hydrophobic residues residing in the catalytic pocket, namely Val 66 and Ile 174 (51). Mutations of these residues to Alanine resulted in resistance to binding of a number of inhibitors while retaining catalytic activity. Structural analysis of CX-4945 binding to CK2 revealed additional interactions with His 160 (161 in the case of α') (48). With the additional substitution of His 160 to either glutamic or aspartic acid in combination with V66A/I174A even greater resistance to CX-4945 treatment can be achieved without significantly altering catalytic activity. To exploit these mutants for the investigation of the phenotypic effects of CK2 inhibitors, we have engineered human osteosarcoma U2-OS cell lines expressing the CK2 α V66A/I174A/H160D (Inhibitor-refractory) mutants under the control of tetracycline using the Flp-in Trex system (52). These inhibitor resistant cell lines have been shown to be demonstrably less sensitive to many CK2 inhibitors, with the greatest resistance to treatment with CX-4945. These cell lines can now be used as tools to distinguish off-target effects of CK2 inhibitors and provide a platform to undertake a global analysis of CK2 dependent cellular signaling pathways.

1.9 Mass Spectrometry Based Proteomics

The field of proteomics encompasses diverse techniques that allow for the analysis of different aspects of protein structure and function. Of the many proteomic

techniques available, mass spectrometry has emerged as the leading method for the analysis of proteins in their native states (53). Among the most attractive attributes of mass spectrometry based proteomics are its unparalleled ability to acquire high-content quantitative information of enormously complex biological samples such as human cells or tissues (54). Current instrumentation allows for rapid analysis, yielding the identification and quantitation of thousands of proteins in a limited amount of time (55). There are two popular approaches to mass spectrometry-based proteomics designated as either “bottom-up” or “top-down” approaches. Top down proteomics studies proteins as intact entities. This has the advantage that all protein modifications should in principle occur on the same molecule and can be measured together (56). However, bottom-up proteomics, in which peptides are generated from the enzymatic digestion of proteins has become experimentally and computationally more reliable and has seen more widespread use among proteomics workflows (56). There are a few permutations to bottom-up proteomics workflows, nevertheless they follow the same general workflow. Proteins are first extracted from their sources (human tissue, cell culture, bacterial culture etc.) and subsequently digested with a sequence specific protease, typically trypsin or Lys-C. The peptide mixture is then separated by reverse-phase liquid chromatography columns such as C18. Peptides are eluted from the column using a gradient of increasing concentrations of organic solvent, thereby separating the peptides based on their hydrophobicity and then ionized via electrospray ionization (57). The ionized peptides are then sent to the vacuum portion of the mass spectrometer, where they are fragmented and measured based on their mass to charge (m/z) ratio. The most common method for data acquisition in bottom-up proteomics is data-dependent acquisition (DDA). Data are acquired in DDA

in two stages. First, mass spectra of the most abundant ion species (precursor ions) co-eluting at a specific point in the gradient are recorded at the MS1 level. The selected precursor ions, typically the most abundant, are then transferred to a collision cell where they are further fragmented via collision-induced dissociation (CID) and detected in a second mass analyzer (MS2). The differences in mass observed between fragment ions allows for the sequencing and identification of the precursor ion. This information can then be searched against a database for statistical validation of the sequence. The overall aim of the bottom-up approach is to achieve unbiased and complete coverage of the proteome. This contrasts with targeted proteomic workflows such as selected reaction monitoring (SRM). The aim of targeted proteomics workflows is to produce a reliable, reproducible streamlined acquisition of a subset of known peptides of interest. Typically, these peptides are identified from previous global proteomic experiments (an in depth review can be found in ref 58).

1.10 Quantitative Proteomics

Mass spectrometry is not inherently quantitative. Proteolytic peptides exhibit a wide range physico-chemical properties that have an impact on their ability to be reliably quantified (58). To overcome this limitation, several strategies have been devised to obtain quantitative information from mass spectrometry experiments. In general, these strategies involve differentially labelling treatment groups at either the protein or peptide level. When lysates are combined, and analyzed by mass spectrometry, peptides deriving from different treatment groups can be distinguished by computational approaches and yield quantitative information in the form of intensity ratios. Several strategies exist for

labelling at the peptide level. For example, isobaric tags for absolute and relative quantitation (iTRAQ)(59), tandem mass tags (TMT) (60), and dimethyl labelling (61) are all commonly used. Labelling can also occur at the protein level using biosynthetic in vivo labeling of the biological sample of interest. Stable isotopic labelling of amino acids in cell culture (SILAC) involves in vivo labelling of proteins by culturing biological samples from separate treatment groups in media supplemented with arginine and lysine containing either ^{13}C or ^{15}N “heavy” isotopes (62). Using an amino acid specific protease such as trypsin or Lys-C, which cleave at the C-terminus of arginine and lysine residues, will theoretically result in every digested peptide containing an isotopic label. By using media containing three isotopically distinct forms of arginine and lysine, triple encoding SILAC allows for the comparison of three cell populations in a single experiment. In this type of workflow, samples from three populations are combined at the protein (lysate) level prior to digestions and subsequent sample preparation. This ensures peptides from all conditions are treated in the same manner and changes in the relative abundance of each peptide are due solely to experimental treatment rather than technical variability. SILAC labelled peptides will elute from HPLC at the same time since the isotopically labelled amino acids are chemically identical to their non-labelled counterparts. The peptides are only distinguishable based on a predictable mass difference due to the presence of heavy labelled amino acids. The abundance of each peptide can then be determined through relative quantitation. MaxQuant, a freely available mass spectra analysis software can detect the three-dimensional characteristics of a SILAC pair at the MS1 level using mass/charge ratios, signal intensity and elution time (63, 64). Thus the combination of computational software and in-vivo labeling

allows for the accurate identification and quantitation of thousands of peptides detected in an LC-MS/MS acquisition.

1.11 Phosphoproteomics

Phosphorylation is one of the most prevalent post-translational modifications. It has been estimated that upwards of 30% of cellular proteins are phosphorylated at any given time (65). Discerning the complex networks and functions coordinated by phosphorylation is a challenging endeavour, requiring knowledge of specific amino acid modifications with spatial-temporal resolution. Mass spectrometry has emerged as the leading tool for investigating global post translational modifications. Naturally, mass-spectrometry based phosphoproteomics has become the standard approach for investigating protein phosphorylation. Several challenges face the study of phosphorylation in cells. In particular, the low stoichiometry of phosphopeptides relative to non-phosphorylated peptides often results in their gross underrepresentation in complex mixtures (66). In addition, there are limitations to the data-dependent acquisition method for the analysis of phosphopeptides. As previously discussed, DDA tandem mass spectrometry routines select precursor ions for fragmentation based on ion signal intensity. In situations where the stoichiometry of phosphorylation at a given site is less than 10%, the ion intensity of the non-phosphorylated peptide will always dominate the survey mass spectrum and be selected for MS2 (67). This especially applies to complex mixtures, for example a triplex-SILAC experiment, where the number of peptides eluted from chromatography already exceeds the number of peptides that can be sequenced by the mass spectrometer in the same time frame. Consequently, phosphopeptide enrichment

strategies are used to address these limitations, and enable the accurate identification and quantification of phosphorylated peptides. One common enrichment strategy is the use of metal oxide affinity chromatography (MOAC) using TiO₂ (68). TiO₂ selectively enriches for phosphorylated peptides by forming a bridging bidentate surface complex (69). This method has the advantage of being highly selective for phosphorylated peptides compared to other methods, and is relatively quick with limited sample handling required (70). Used in combination with a quantitative label such as SILAC, the relative comparison of the abundance of phosphopeptides between treatments can enable the quantitation and localization of a given phosphorylated residue (71). This information can then be analysed using bioinformatics workflows that can potentially determine kinase-substrate relationships as well as information regarding the cellular signaling context.

1.12 Thesis Objective and Rationale

Although CK2 has shown promise as a clinical target, questions remained unanswered as to the precise mechanisms by which CK2 operates and how it can best be targeted for the treatment of disease including cancer. Advances in large-scale proteomics and the development of computational platforms for the analysis of proteomic data have enabled the exploration of cellular responses to kinase inhibition on a global scale. Several phosphoproteomic studies have demonstrated decreases in phosphorylation in sites conforming to the CK2 consensus sequence. For example, a study investigating MEK inhibitor resistance in BRAFV600E cells revealed an increase in the number of phosphorylation sites in acidophilic sequences, 50% of which conformed to the CK2

consensus sequence (72). Not only do these types of study suggest an important role for CK2 in oncogenic signalling, they also provide a proof of principle that physiological substrates of CK2 are amenable to detection by mass spectrometry based phosphoproteomic techniques. Although it is possible that many of these sites are direct substrates of CK2, it is impossible to assign any of them as “bonafide” substrates in the absence of direct manipulation of CK2. Chemical inhibition of CK2 has become the most widely used approach in investigating its role in cellular signalling events. However, the small-molecule inhibitors used in these studies have not been systematically evaluated for CK2 specificity using unbiased methods in a cellular context. To address this limitation, inhibitor refractory mutants of CK2 α catalytic subunit have been generated by manipulating the ATP-binding pocket while maintaining catalytic activity. These mutants have demonstrated the ability to evade inhibition by CK2 specific inhibitors, and can serve as a tool to validate biological processes related to CK2 as well as distinguish between on and off-target effects of small molecule inhibitors. Similar approaches have been used to evaluate the specificity of kinase inhibitors. For example, Scutt et al (2009) developed inhibitor resistant mutants of Aurora kinase A that were integrated into cell lines under inducible expression (73). In doing so they were able to validate the specificity of several small-molecule inhibitors targeting Aurora kinase A and simultaneously uncovered information regarding its mechanism of action.

Applying proteomic and phosphoproteomic strategies in combination with cell lines expressing inhibitor refractory mutants of CK2 would be invaluable in assessing the specificity of CK2 inhibitors as well as uncovering novel substrates of CK2 which could serve as activity biomarkers. Given the emergence of as a therapeutic target and the

advancement of CX-4945 through the clinical pipeline, an unbiased investigation of CX-4945 on a global scale is also warranted. Characterization of CX-4945 in the presence of both wild-type and inhibitor refractory mutants of CK2 has the potential to highlight CK2-dependent effects on cellular processes and reveal potential off-targets of CX-4945.

In this study, cell lines engineered to harbour inhibitor refractory mutants of CK2alpha as well as wild-type CK2alpha under the inducible control of tetracycline were characterized prior to their phosphoproteomic application. The exogenously expressed subunits were found to interact with the existing cellular machinery. Time course experiments using the inhibitor refractory cell lines demonstrated robust ability to evade inhibition by CX-4945, and resulted in the identification of a window of time where CK2 activity could be recovered while also preceding the activation of cell death pathways. Phosphoproteomics analysis of the cell lines expressing inhibitor refractory CK2 or wild-type CK2 was then performed to profile the CK2 dependent effects of inhibition by CX-4945. Using a quantitative proteomic “triple-SILAC” strategy in Flp-U2OS cells harbouring the inhibitor refractory and wild-type CK2alpha subunits, we were able to uncover novel substrates of CK2 and distinguish several off-target effects of CX-4945. Overall, this investigation uncovered novel evidence for potential mechanistic roles for CK2 in cellular signaling. several novel phosphoproteins were identified in which the inhibitor refractory CK2alpha was able to restore phosphorylation to a significant degree, providing a panel of potential biomarkers with which the activity of CK2 could be monitored in various cellular contexts. In general, this investigation revealed the broad impact on the phosphoproteome as a result of treatment with CX-4945. The proteomic interrogation revealed a number of novel substrates that could be used to monitor the

activity of CK2 in cells, as well as revealing the impact of CK2 inhibition by CX-4945 on the activity of several other kinases following kinase-substrate enrichment analysis.

Therefore this investigation outlines both a mechanistic role for CK2 in signaling processes, and CK2-independent effects that occur as a result of treatment with CX-4945.

2 Experimental Methods

2.1 Cell Culture, Lysis & Western Blotting for Sustained Induction Experiments

Flp-U2OS cells (provided by Karmella Haynes) expressing inhibitor refractory mutants and wild-type CK2alpha were cultured in Dulbecco's modified Eagle's medium (DMEM) (Corning) containing 10% FBS, penicillin (100 U/mL), streptomycin (100 µg/mL), hygromycin B (150 µg/mL) and blasticidin (15 µg/mL). Induction of the exogenous proteins relied on the addition of tetracycline (1 µg/mL) on a 10 cm dishes. Cells were cultured in media containing tetracycline for and passaged every day for 5 days. Following each passage 50% of the cells were collected and lysed. Cells cultured free of tetracycline were passaged and lysed in parallel. Media was vacuum-aspirated and cells were washed with ice cold PBS, followed by lysis on ice using Tris Lysis Buffer (50 mM Tris pH 7.5, 150 mM NaCl, 1% NP-40, 0.1 Deoxycholic Acid) with additional protease and phosphate inhibitors (1 mM PMSF, 7 µg/ml Pepstatin A, 20 µg/ml Leupeptin, 2.9 µg/ml Aprotinin, 1 µM Okadaic acid, 1 µM Microcystin, 5 mM NaF, 1 mM sodium orthovanadate). Total cell lysates were then spun for 10 minutes at 13,000 x g at 4 °C. The supernatant was retained and protein concentration was determined using BCA protein assay (Thermo). Equal amounts of each sample (10 µg) was loaded per lane and separated by SDS-PAGE. Proteins were transferred to PVDF membrane (Millipore) using a wet-transfer apparatus (Bio-Rad) at 400 mA for 60 minutes at 4 °C followed by

incubation in blocking buffer (LI-COR Biosciences) for 30 minutes. Primary anti-CK2alpha/alpha' antibodies raised against the c-terminal portion of CK2alpha', a region of the protein containing substantial overlap with the c-terminal of CK2alpha and is thus able to detect both subunits as well as the HA-tagged CK2alpha were incubated at room temperature for 1 hour in 3% BSA-PBST. Secondary antibody GAR-800 (926-32211) was used with incubation for 45 minutes. Following 3 x 5 minute washes with PBST, membranes were scanned using an Odyssey scanner (LICOR-Biosciences) at 700 nm and 800 nm wavelengths. Raw data scans were loaded into ImageStudioLite (LICOR-Biosciences) and exported as TIFF images.

2.2 Inhibitor Time-courses

Flp-U2OS cells (Karmella Haynes) expressing inhibitor refractory mutants and wild-type CK2-alpha were cultured in Dulbecco's modified Eagle's medium (DMEM) (Corning) containing 10% FBS, penicillin (100 U/mL), streptomycin (100 µg/mL), hygromycin B (150 µg/mL) and blasticidin (15 µg/mL). Cells were seeded to 80% confluency on 6-well dishes. Cells were then treated with either 1 µM Staurosporine or 50 µM CX-4945 for various lengths of time. Following the time course, cells were lysed as described in section 2.1. Western blotting was done with anti-PARP antibodies in 3% BSA/TBST to detect the initiation of apoptosis

2.3 Immunoprecipitation

Flp-U2OS cells expressing inhibitor refractory and wild-type CK2 alpha were cultured as described in section 2.1 in the presence of tetracycline for 48 hours to induce

exogenous protein expression. Cells were washed twice with cold PBS and lysed as described in section 2.1. Cell extracts were centrifuged and collected using the same parameters as described above. Supernatants were collected and protein concentrations were determined by BCA protein assay (Thermo) using BSA as a standard. Next, 300 μ g of protein from each cell line was aliquoted into fresh tubes and normalized for volume. Supernatants were pre-cleared by adding 30 μ L of 50% Protein-G slurry beads. Pre-cleared lysate was spun down and supernatants were collected. Then, 30 μ L of a 50% slurry of Protein-G Sepharose beads (Sigma) and 1 μ L of anti-CK2 β antibody (BAbCo) were added to protein supernatants. The immunoprecipitations were allowed to tumble for 1 hour at 4 °C. The beads were then collected by centrifugation and washed four times with Tris Lysis Buffer (same as used for lysis) and finally suspended in 40 μ L Laemmli buffer with 10% β -mercaptoethanol. The anti-CK2 β and CK2 α -HA immunoprecipitations were then analyzed by western blot. To monitor complex formation between exogenous CK2- α and endogenous CK2 β , immunoprecipitates were blotted using anti-HA 3F10 antibody (Roche).

2.4 SILAC Medium Formulation

SILAC-droupout DMEM (Wisent) lacking L-arginine, and L-lysine was supplemented with isotope-encoded L-arginine (Arg-6) ($^{13}\text{C}_6$) and L-lysine (Lys-4) (4,4,5,5-D $_4$) (Silantes) at respective concentrations of 86.2 mg/L (0.398 mM) and 61.16 mg/L (0.274 mM) to create a “medium labelled” medium. “Heavy” medium was created by supplementing the SILAC-dropout DMEM with isotope encoded “heavy” L-arginine (Arg-10) ($^{13}\text{C}_6$, $^{15}\text{N}_4$) and “heavy” L-lysine (Lys-8) ($^{13}\text{C}_6$, $^{15}\text{N}_2$) at respective

concentrations of 87.7 mg/L (0.397 mM) and 52.4 mg/L (0.274 mM). “Light” medium was created using the SILAC-dropout DMEM and supplementing it with unlabeled L-arginine (R0) (83.9 mg/mL) and L-lysine (K0) (60.04 mg/mL). All media used for SIAC studies were supplemented with 10% 10kDa-dialyzed FBS (Wisent), penicillin (100 U/mL), streptomycin (100 mg/mL) and L-proline (400 mg/mL) (Cambridge Isotope Laboratories Inc.) in order to prevent arginine to proline conversion (Bendall et al., 2008). Media was filter sterilized prior to use for cell culture.

2.5 SILAC Incorporation of Flp-U2OS Cells

Flp-U2OS cells expressing wild-type CK2-alpha were adapted over a period of 7 days with 3 sub-passages after being switched to “medium” SILAC medium. An Aliquot of protein lysate from “medium” labelled cells was precipitated by chloroform/methanol extraction. Precipitated pellets were resuspended in 500 µL TFE (2,2,2-Trifluoroethanol) Digestion buffer (10% TFE, 100 mM ammonium bicarbonate) with sonication for 15 seconds or until a homogenous suspension was formed. Trypsin-Lys-C (Promega) at 200:1 (w/w) was used for the first 4-hour digestion step and Trypsin at 100:1 (Pierce) was used for the overnight incubation step. Digested peptides were desalted using a C18 StageTip (Empore). LC-MS/MS parameters for acquisition are discussed in section 2.6 with data acquisition performed on an Orbitrap Elite mass spectrometer. Raw spectra were analyzed using MaxQuant v1.5.3.8 and searched against the Swissprot-Uniprot sequence database (homo sapiens taxon, accessed on December 26, 2015). Samples were searched using a multiplicity set to 2 with “medium” labels selected as Arg6 and Lys4. Mass tolerances were set to 4.5 ppm for the parent ion mass (MS) and 0.5 Da or the

fragment ion mass (MS/MS). The minimum number of amino acids in a peptide was set to 7, with a peptide spectrum match (PSM) and protein match set to 1% FDR and protease selectivity for Trypsin/P. A maximum number of 3 missed cleavages was selected. The number of variable modifications per peptide was 5, with methionine oxidation (+15.9949), protein N-terminus acetylation (+42.0105), asparagine and glutamine deamidation (+0.9840 Da) selected. Cysteine carbamidomethylation (+57.0215) was set as a fixed modification. Re-Quantify option was turned on. The minimum score for modified peptides was set to 40, and the decoy-database setting was “Revert.” Output data from MaxQuant was then loaded into Perseus version 1.5.2.6. The “evidence.txt” file was used to extract information about peptides that were quantified in MS1 and identified in MS2, from which reverse hits and contaminants were removed. The heavy and light intensity values from MS1 quantitation were used to calculate H/L ratios. Two formulae were applied to calculate the incorporation for each peptide: H/L ratios larger than 1 were calculated with $(100 - (1/\text{ratio}) * 100)$, and ratios less than 1 were calculated with $(\text{ratio} * 100)$. The median of all incorporation values for each individual SILAC pair was calculated and represents the incorporation efficiency for the labeled amino acids. The process was repeated for the incorporation of “heavy” labelled Arg10 and Lys8.

2.6 CX-4945 Treatment and Lysis of SILAC Flp-U2OS Cells

Flp-U2OS cells expressing wild-type and inhibitor-refractory mutants of CK2-alpha were cultured in “medium” and “heavy” SILAC medium respectively. “Light” labelled cells expressing wild-type CK2alpha were cultured as a control dish. Exogenous

proteins were induced by the addition of 1 $\mu\text{g/mL}$ tetracycline and cells remained in culture for 48 hours until 80% confluent. Following the 48-hour induction period, cells were treated with 30 μM CX-4945 (MedKoo Biosciences) for 4 hours, with light labelled cells expressing CK2 α treated with DMSO vehicle. Experiments were carried out in biological quadruplet. Following treatment, media was vacuum-aspirated and cells were washed with ice cold PBS followed by lysis on ice in 1 mL of GdmCl lysis buffer (6M GdmCl, 100 mM Tris pH 8.5, 10mM TCEP, 40 mM CAA (Chloroacetamide)). Lysates were then heated for 5 minutes at 95 $^{\circ}\text{C}$, cooled on ice for 15 minutes, sonicated for 2 x 15 seconds and heated again at 95 $^{\circ}\text{C}$ for 5 minutes. Lysates were then spun for 10 minutes at 13 000 x g at 4 $^{\circ}\text{C}$. The supernatant was retained and protein concentration was determined using a Bradford assay (Bio-Rad). Samples were frozen at – 80 $^{\circ}\text{C}$ until processing.

2.7 LC-MS/MS Data Acquisition

Samples were analyzed using an Orbitrap Elite Hybrid Ion Trap-Orbitrap mass spectrometer. Samples were injected using a NanoAcquity UPLC (Waters) onto a Symmetry C18 trapping column (20 mm x 180 μm i.d., 5 μm , 100 \AA) at a flow rate of 10 $\mu\text{L/min}$ in 99% mobile phase A (0.1% FA (v/v), 1% mobile phase B (0.1% FA (v/v) in ACN) for 4 minutes. Samples were then separated on a NanoAcquity Peptide BEH C18 analytical column (250 mm x 75 μm i.d., 1.7 μm , 130 \AA) at a flow rate of 300 nL/min by a linear gradient of increasing mobile phase B from starting condition 7.5% to 25% for 180 minutes, followed by 25% to 32.5% for 40 minutes, and culminating at 60% at 240 minutes. Separated peptides were ionized using a nano-Electro Spray Ionization source

connected to the analytical column by a fused-silica capillary emitter (New Objective). Ionized peptides were analyzed using a Orbitrap Elite Hybrid Ion Trap-Orbitrap mass spectrometer (Thermo Scientific) operated by Thermo XCalibur (software version 2.7.0.1094) in data-dependent mode. MS1 scans were performed at 120,000 resolution, scanning from 400 – 1450 m/z with AGC set to 5×10^2 ions and an isolation window of 1.0 m/z. The top 20 most abundant ions were selected for MS2. A lock mass ion was enabled for 445.120025 m/z. Maximal injection time for MS1 acquisition was 200 ms and 50 ms for MS2. Peptide ions were fragmented using CID with NCE set to 35% with activation time set to 10 ms and a Q value of 0.25. Data-dependent MS2 scans were acquired in the linear ion trap using rapid scan selection, with a dynamic exclusion window of 60 seconds. Four biological replicates were analyzed without technical replicates. Raw mass spectra files were analyzed in MaxQuant version 1.5.3.8 and searched against the Swissprot-Uniprot sequence database (homo sapiens taxon, accessed on December 26, 2015). Samples were searched using a Multiplicity set to 3, with “medium” labels selected as Arg6 and Lys4 and “heavy” labels selected as Arg8 and Lys10. Mass tolerances were set to 4.5 ppm for the parent ion mass (MS) and 0.5 Da for the fragment ion mass (MS/MS). Mass tolerances were set to 4.5 ppm for the parent ion mass (MS) and 0.5 Da for the fragment ion mass (MS/MS). The minimum number for amino acids in a peptide was set to 7, with a peptide spectrum match (PSM) and protein match set to 1% FDR and protease selectivity for trypsin/P. A maximum number of 3 missed cleavages was chosen. The option for second peptide search was selected, as well as the use of “Match Between Runs” for respective pairs of samples between biological replicates, using default parameters. Raw mass spectra files were defined as separate

groups using the experimental setup option. Cysteine carbamidomethylation (+ 57.0215 Da) was set as a fixed modification. For phosphopeptide samples, 6 variable modifications were chosen, with methionine oxidation (+15.9949 Da), protein N-terminus acetylation (+42.0105 Da), asparagine and glutamine deamidation (+0.9840 Da) and serine, threonine, and tyrosine phosphorylation (+79.9663) selected. For proteome samples the maximum number of variable modifications was set to 5, and phosphorylation as a variable modification was excluded from these samples. The minimum score for modified peptides was set to 40, and the decoy-database setting was “Revert.” For quantification of protein groups, unmodified peptides and those with carbamidomethylation, methionine oxidation, protein N-terminus acetylation or asparagine and glutamine deamidation were included. Peptides for which the corresponding heavy or medium modified peptide were not quantified were excluded from the protein.groups quantitation. Output data from MaxQuant was then loaded into Perseus version 1.5.2.6. For proteome data analysis, the “proteinGroups.txt” file was first processed to remove entries marked as reverse decoy database hits, contaminants, and protein identifications that were only matched to modified peptides. MaxQuant-generated normalized ratios were utilized, and the log base 2 of the normalized ratios was calculated for each protein. Proteins were considered identified in each biological replicate if identified in all biological replicates. For the analysis of the phosphoproteome data, the “Phospho(ST)Sites.txt” file was first processed to remove entries marked as reverse decoy database hit and contaminants, and filtered to only contain phosphorylation sites with localization probability greater than 0.75. Phosphorylation sites were expanded in Perseus to obtain information from instances of quantified sites being derived from

singly, doubly and triply-phosphorylated peptides. Rows where no quantification was present were removed, and phosphorylation sites were considered quantified in each biological replicate if they were identified in all biological replicates.

2.8 Sample Digestion and Phosphopeptide Enrichment

Prior to sample processing 1mg of protein lysate derived from light labelled cells treated with DMSO, medium labelled wild-type expressing cells treated with CX-4945, and heavy labelled cells expressing the inhibitor-refractory CK2-alpha were combined for a total of 3 mg of lysate for each biological replicate resulting in 4 samples. Samples were then processed by protein precipitation and digested following the methods described in section 2.4. The peptide solution was then cleared at 13 000 x g for 15 minutes and was then transferred to clean tubes. TiO₂ beads were prepared by resuspension into Loading buffer (80% ACN, 6% TFA). TiO₂ beads were weighed out at a ratio of 10:1 (TiO₂ beads/protein, w/w) for enrichment. The bead suspension was then transferred to the cleared peptide solution. Prior to addition, a small aliquot of the peptide solution was removed for proteome analysis. The TiO₂-peptide solution was then allowed to tumble at room temperature for 20 minutes. Beads were then collected by centrifugation for 1 minute at 3,500 x g at room temperature, the supernatant was saved and stored at – 80 °C. Non-specifically bound peptides were washed from the TiO₂ beads by resuspension in 500 µL Wash buffer (60% ACN, 1% TFA) and transferred to clean 2 mL tubes, collecting any remaining beads with a second 500 µL of Wash buffer. Beads were then vortexed and centrifuged for 1 minute at 3,500 x g at room temperature and supernatant was discarded by aspiration. Pelleted beads were washed an additional 4 times with 1 mL

Wash buffer, incubating each wash for 30 seconds and vortexing. After the final wash, 100 μ L Transfer buffer (80% ACN, 0.5% Formic Acid) was added to the beads and vortexed for resuspension. The beads were then transferred on top of a C18 (single layer) StageTip, which was then centrifuged for 5 minutes at 500 x g at room temperature, or until no liquid remained in the StageTip. Phosphopeptides were eluted with the addition of 100 μ L Elution buffer (40% ACN, 15% NH_4OH (25%, HPLC grade)) and centrifuged for 3 minutes at 500 x g or until no liquid remained. Eluates were collected in 1.7 mL low-retention Eppendorf tubes. Samples were concentrated in a Speed Vac for 15 minutes at 45 °C or until ~ 20 μ L remained and 10% TFA was immediately added to the samples. Phosphopeptides were desalted on StageTips with 4X layers of SDB-RPS (pre-calibrated). Samples were loaded onto StageTips and centrifuged for 3 minutes at 500 x g or until no liquid remained. Peptides were then washed with 200 μ L Wash buffer (0.2% TFA) four times. Peptides were then eluted by the addition of 100 μ L SDS-RPS Elution buffer (80% CAN, 5% NH_4OH (25% HPLC grade)). Phosphopeptides were collected into clean low-retention Eppendorf tubes by centrifugation for 5 minutes at 500 xg at room temperature or until no liquid remained. Eluent was immediately placed in SpeedyVac for 30 minutes at 45 °C or until ~ 10 μ L remained. 0.1% Formic acid was immediately added for acidification. Sample concentrations were determined by NanoDrop A280 and transferred to glass LC-MS vials and stored at -80 °C until data acquisition.

2.9 Data Analysis

Statistically significant phosphorylation sites that responded to CX-4945 treatment and the inhibitor refractory mutants of CK2-alpha were determined by one-sample Student's t-test with multiple hypothesis correction using Benjamini-Hochberg $FDR = 0.05$. Phosphorylation sites were filtered based on selection criteria outline in section 3.2. The putative upstream kinases of selected phosphorylation sites were generated using KinomeXplorer(74) for kinase prediction and filtering. Phosphoproteomic and proteomic data were filtered using the R framework (v3.2.3). Data visualization was done using the ggplot2 package within the R framework. Phosphoproteomic datasets of the wild-type and inhibitor-refractory expressing cell lines were compared using the Kinase Perturbation Analysis (75) package within the R framework. PHOXTRACK (76) was used to identify kinase-substrate relationships. The Phosphositeplus (77) database was queried with uploaded mean log2 ratios of phosphorylation sites from each dataset. An unweighted Kolmogorov-Smirnov running sum statistic was calculated for the query list of phosphorylated sites with the number of permutations set to 10,000. Gene ontology analysis was done using Panther Gene list analysis (78). Selected genes from the list of phosphosites were uploaded into the Panther framework, *Homo sapiens* were selected as the organism, and functional classification was selected as the analysis. Motif analysis was performed using the Motif-X software from Harvard University (79, 80).

3 Results

3.1 Characterization of U2OS Cell Lines Expressing Wild-type and Inhibitor-Refractory Mutants of CK2-alpha

Previously, U2OS osteosarcoma cells were engineered to harbour tetracycline inducible inhibitor refractory mutants of the catalytic CK2alpha, as well as cells harbouring the wild-type CK2alpha, using the Flp-in Trex system developed by Karmella Haynes (52). For these cell lines to be used as a tool of study, we first had to determine the parameters of their exogenous protein induction capabilities, the ability of the exogenously expressed CK2alpha to interact with the existing pool of CK2, as well as the ability of the inhibitor refractory mutants to escape inhibition from CK2 inhibitors. First, exogenous proteins were induced in the engineered U2OS cells harbouring either the HA-tagged inhibitor refractory and wild-type by the addition of tetracycline (1µg/ml), and monitored for a period of 1-5 days, after which cell lysates were collected and separated by SDS-PAGE. Expression of the exogenous CK2 subunits as well as their expression levels relative to that of the endogenous protein was detected by western blotting using an anti-CK2alpha/alpha' antibody capable of detecting both catalytic subunits as well as the exogenous HA-tagged subunits. Blotting revealed consistent expression over the five-day period for each of the cell lines. Expression appears to plateau after 48 hours, indicating a steady state is reached at that time point. Although there is robust expression after 24 hours of induction, exogenous levels are approximately 2-fold higher after 48 hours.

Given this observation, all subsequent induction experiments were done after 48 hours of induction. Quantification of the upper most band (48kDa) compared to the band corresponding to exogenous CK2alpha shows that they are expressed at roughly equal levels for both the inhibitor refractory and wild-type exogenous CK2. Interestingly, over the course of the 5-day period there appears to be a significant reduction in the levels of CK2alpha', suggesting a possible intrinsic threshold for the levels of catalytic CK2. In addition, sum intensities of exogenous CK2alpha, and endogenous CK2alpha/alpha' remain relatively equal throughout the 5-day induction period. These observations suggest that the total pool of catalytic CK2 remains the same after two days of induction, with the exogenously expressed protein replacing that of the endogenous.

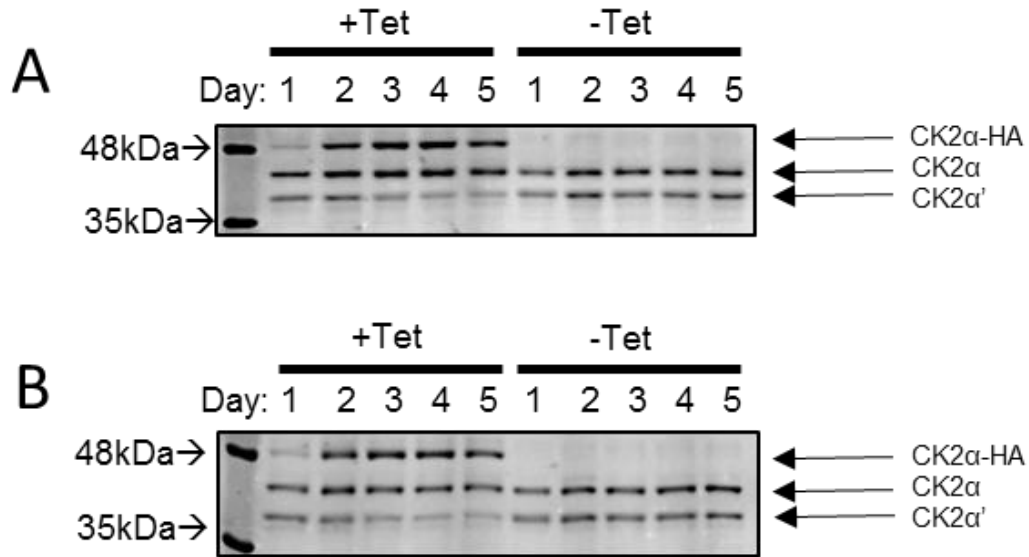


Figure 3. Sustained Exogenous Expression of Wild-type and Inhibitor Refractory CK2- α . Expression of exogenous wild-type CK2 α -HA (A) and Inhibitor Refractory CK2 α (B) induced by the addition of tetracycline was monitored over a period of five days. Expression was detected by western blot using an anti-CK2 α / α' antibody capable of detecting exogenous CK2 α -HA, endogenous CK2- α and α' . Control cells were maintained in media free of tetracycline.³

Several aspects of CK2's functionality in cells such as substrate specificity and stability are dependent upon complex formation between the catalytic subunits and regulatory CK2beta subunit (81, 82). To determine whether the exogenously expressed CK2 forms a complex with endogenous CK2beta, immunoprecipitation assays were performed. Following an induction period of 48 hours, endogenous CK2beta was immunoprecipitated using an anti-CK2beta Antibody. Western blotting with anti-HA 3F10 shows that the exogenously expressed CK2alpha was present in the lysate and in the immunoprecipitates (Figure 4). Blotting revealed that CK2beta was isolated with both the exogenously expressed inhibitor refractory mutant and wild-type protein, indicating the incorporation of the proteins into the holoenzyme complex. In addition, time-courses with CX-4945 following expression of the inhibitor refractory mutants have demonstrated that it is capable of restoring phosphorylation of the S2/3/4/8 sites on CK2 β (Supplementary Figure 1), whose phosphorylation is indicative of holoenzyme formation (83).

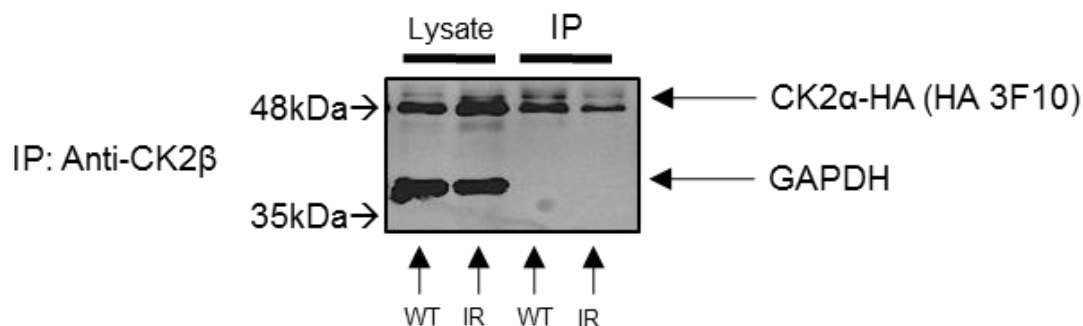


Figure 4. Exogenous CK2-alpha forms complexes with endogenous CK2β.

Exogenous proteins were induced in Flp-U2OS cell lines harbouring both wild-type and inhibitor refractory mutants of CK2-alpha by the addition of 1µg/ml tetracycline for 48 hours prior to cell harvest. Immunoprecipitation of endogenous CK2β was performed using an anti-CK2β antibody. Immunoprecipitates were boiled and resolved via SDS-PAGE. Complex formation with exogenous CK2alpha-HA was detected by western blotting using an anti-HA antibody. Western blotting using anti-GAPDH antibody serves as a control to indicate the absence of cell lysate in the immunoprecipitation lanes.

The ability of the inhibitor refractory mutants to escape inhibition by CK2 inhibitor CX-4945 had until this point only been determined via in vitro assays using recombinant protein. Previous experiments determined that treatment with 30 μ M of CX-4945 is the optimal concentration in U2OS cells achieving maximal inhibition of CK2 (Supplementary Figure 2). To determine the ability of the inhibitor resistant mutant to escape inhibition following CX-4945 treatment, exogenous proteins were induced in the engineered cells (inhibitor refractory and wild type) for a period of 48 hours, followed by 30 μ M CX-4945 treatment which was sustained for either 0, 2, 4, 8, or 24 hours (Figure 5). Control cells were treated with equal volume of the vehicle DMSO over the same time points. CK2 inhibition was assessed by western blotting with phospho-specific antibodies raised against established CK2 phosphorylation sites. In particular, pEIF2S2 S2 is a dynamic marker of CK2 activity for which an antibody has been raised. CX-4945 treatment resulted in a roughly linear decrease in phosphorylation of EIF2S2 at the S2 site over the length of the time course for both cell lines (Figure 5). Comparing the treatments between the inhibitor refractory and wild-type cell lines, it was evident that phosphorylation of EIF2S2 at S2 was decreased to a much lesser extent in the inhibitor refractory cell line at 4, 8, and 24 hours following CX-4945 treatment. This serves as confirmation that the inhibitor refractory cell lines can be used to recover CK2 activity in the presence of CX-4945 in a cellular context. Additionally, this information will be used when determining the conditions for subsequent proteomic experiments

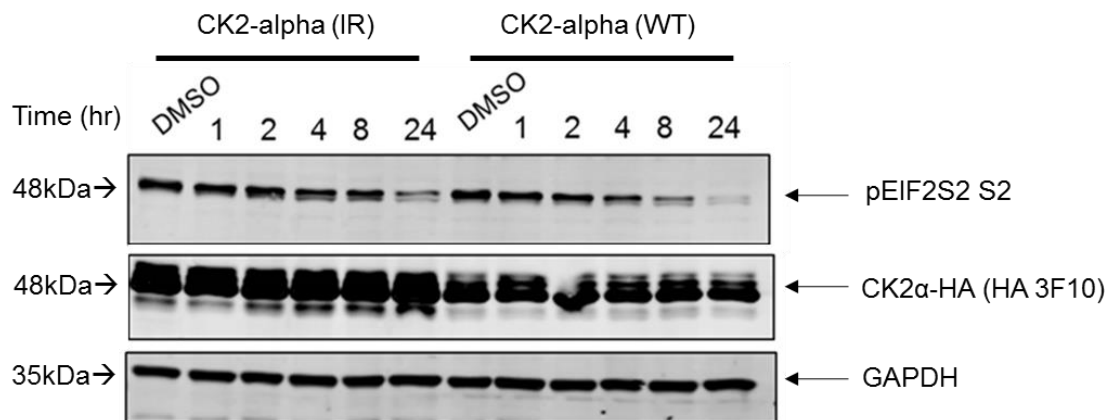


Figure 5. Time-Course Treatment of Engineered Flp-U2OS cells with 30μM CX-4945. Exogenous proteins were induced in Flp-U2OS cells engineered to harbour tetracycline inducible HA-tagged inhibitor refractory (IR) and wild-type (WT) CK2-alpha by the addition of 1 μg/ml tetracycline for 48 hours. Cells were then treated with 30μM CX-4945 for intervals up to 24 hours followed by lysis. Lysates were separated by SDS-PAGE, transferred and western blotted using antibodies against HA-epitope, phospho-EIF2S2 and GAPDH.

3.2 Investigating the CK2 Dependent Phosphoproteome Using Cell Lines Expressing Inhibitor Refractory CK2alpha

Prior to embarking on the analysis of the CK2 dependent phosphoproteome using CX-4945 and inhibitor refractory mutants, the engineered cell lines had to first be adapted in SILAC medium for a period of 7 days and a minimum of 3 sub-passages to ensure cellular proteins were isotopically labelled greater than 95% (62). The SILAC medium formulation used was supplemented with equimolar amounts of proline to prevent arginine to proline conversion (84). Following incorporation of the inhibitor refractory and wild-type Flp-in U2OS cell lines in “heavy” (K8R10) and “medium” (K4R6) media, protein samples were collected, digested, and raw mass spectra was acquired by LC-MS/MS. Mean incorporation efficiency was calculated to be greater than 95%, with the distribution skewed towards 100% incorporation (Supplementary Figures 3 and 4).

Previous experiments have demonstrated that with 30 μ M CX-4945 treatment, the inhibitor refractory mutants can restore phosphorylation at 4, 8, and 24 hrs (Figure 5). The 4-hour time point was selected for the phosphoproteomic analysis to maintain consistency with previously completed proteomic experiments (85). In addition, by treating at the relatively short 4-hour time point, we decrease the chances of activating downstream signalling pathways and reduce the time available for the inhibitor to engage potential off-targets. To ensure that inhibition at 4 hours precedes the activation of cell-death pathways, a time course using 50uM CX-4945 was performed. Activation of apoptotic pathways was detected by western blot using an anti-PARP-1 antibody. CX-

4945 treatment up to 6 hours showed no activation of apoptotic pathways (Supplementary Figure 5).

Following confirmation of CK2 inhibition, recovery of phosphorylation by the inhibitor refractory mutants, and no conflicting activation of cell death pathways, the investigation into the CK2-dependent phosphoproteome was undertaken. Three cell lines, Flp-U2OS-CK2alpha-WT in the “light” K0R0 media, Flp-U2OS-CK2alpha-WT in the “medium” K4R6 media, and Flp-U2OS-CK2alpha-V66A/H160DI174A in the “heavy” K8R10 media, had their exogenously expressed proteins induced by the addition of tetracycline (1ug/ml) for 48 hours. Following the induction of exogenous CK2, the inhibitor refractory (K8R10) and wild-type cell lines (K4R6) were treated with 30 μ M CX-4945 for 4 hours. The third cell line expressing wild-type CK2 was treated with equal volume of the vehicle DMSO for the same length of time after which lysates from all three samples were collected. Next, equal amounts of the heavy, medium, and light lysates were combined and digested with trypsin and Lys-C proteases, followed by desalting and phosphopeptide enrichment. Proteome samples were also retained for analysis by LC-MS/MS. By combining the samples in equal amounts prior to digestion and enrichment, biases in the abundance of phosphopeptides between samples in the experimental and control groups were eliminated. Quantitative analysis by mass spectrometry and downstream analysis of the raw spectra using the MaxQuant software allows for the detection of MS1 features which can compute the relative abundances of the phosphopeptides from the three conditions based on their respective isotopic labels. The MS2 spectrum then confirms the identity of the peptide as well as phosphosite localization. The samples were not fractionated prior to acquisition by LC-MS/MS, with

four biological replicates run in total for both the proteome and phosphoproteome samples (Figure 6). Given that there is much higher biological variability than technical variability, controlling for biological variability with 4 replicates will account for technical variation. As such, no technical replicates were run. The acquisition resulted in the identification and quantification of 1,306 phosphorylation sites and 1,717 proteins groups across all replicates and SILAC labels (Figure 7). Phosphorylation sites were characterized based on their relative fold-changes and statistical significance as determined by one-sample Student's T-test with Benjamini-Hochberg FDR of 0.05 for multiple hypothesis correction. All sites taken into consideration for further analysis are class I phosphorylation sites (localization probability >0.75). Of the sites in the wild-type cell line treated with CX-4945, 69 phosphosites had an increased fold change greater than \log_2 of 1, while 250 sites decreased less than \log_2 fold change of -1 (Figure 7). For sites in the inhibitor refractory cell line, 83 had an increased fold change greater or equal to \log_2 of 1, while 217 had a decreased fold change less than or equal to \log_2 of -1. The broader impact on the phosphoproteome can be seen by volcano plot (Figure 8), where it is evident that treatment with CX-4945 results in dynamic changes. Figure 8 depicts the changes in the phosphoproteome occurring in the wild-type expressing cell line. Confirmation of CK2 inhibition can be seen by the decreased fold change in many known CK2 substrates (Supplementary Figure 6).

3.3 Inhibitor Refractory CK2-alpha Restores Phosphorylation in the Presence of CX-4945

Given the inhibitor refractory cell lines ability to restore phosphorylation to a certain degree in the presence of CX-4945, we anticipate sites phosphorylated by CK2 in the inhibitor resistant phosphoproteome to show an increase (diminished decrease) in phosphorylation relative to the wild-type phosphoproteome. The restoration of phosphorylation in the inhibitor refractory cell line relative to the wild-type is reflected in the Heavy/Medium ratios computed by MaxQuant. To identify phosphorylation sites recovered by the inhibitor refractory mutant, the dataset was filtered for phosphorylation sites that have a decrease in fold change less than or equal to \log_2 of -1 in the wild-type phosphoproteome (Medium/Light ratio), as well as sites that had a Heavy/Medium ratio of at least \log_2 of 0.5, which represents a 25% increase in phosphorylation in the inhibitor refractory compared to the wild-type, as well as statistical significance. Phosphorylation sites that match these criteria are labelled in orange (Figure 8). Of the total phosphosites, approximately 47 of the 1306 were identified as those restored by the inhibitor resistant mutants after filtering (Table 1).

Interestingly, of these 47 phosphosites only one of them (SSB S366) had been previously annotated in the literature as a CK2 site per the phosphosite plus database. Of these sites, only 11 are predicted to be phosphorylated by CK2 as identified using KinomeXplorer. To note are EIF5B Ser214, and AHNAK Ser5857, which show the highest degree of recovery in the inhibitor refractory cell line compared to the wild-type with \log_2 H/M ratios of 2.71 (6.55-fold) and 2.12 (4.35-fold) respectively. Interestingly,

although it is a well-established CK2 phosphorylation site, EIF2S2 Ser2 did not show the greatest magnitude of change upon CX-4945 treatment. While other well-known phosphorylation sites such as TOP2A Ser1377 showed greater extent of inhibition. Additionally, there was no significant extent of recovery in the inhibitor refractory cell line compared to the wild-type cell line for both EIF2S2 and TOP2A sites. These observations suggest preferential de-phosphorylation of individual CK2 phosphorylation sites by phosphatases.

Phosphorylation sites that were selected based on the previously mentioned criteria were then subject to gene ontology analysis to determine the cellular pathways in which they are involved. Several of the sites were involved in the regulation of gene expression, namely RNA processing, nucleic acid metabolic processing and gene expression in general (Figure 9). Analysis of the phosphorylation site motifs showed that the phosphorylated residues were in large part surrounded by acidic amino acids, consistent with the consensus sequence for CK2. This sequence logo also matches that of the sequence logo for all of the CK2 phosphorylation sites in the Phosphositeplus data base (77).

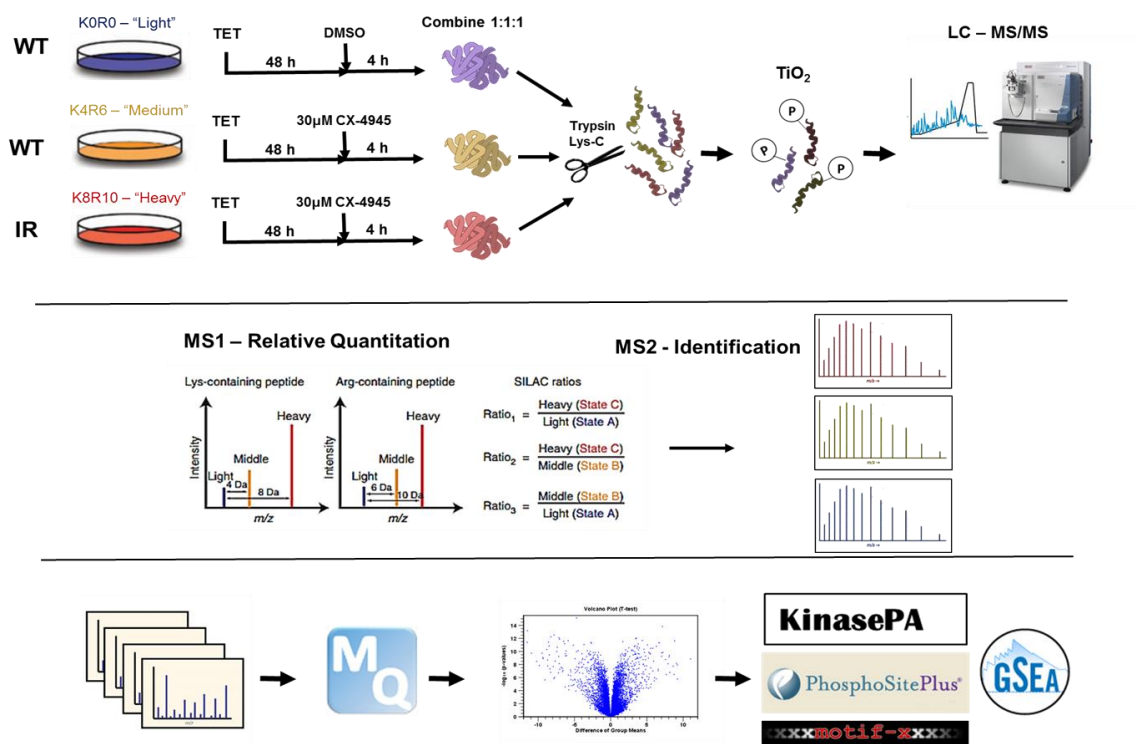


Figure 6. Workflow to Investigate CK2 dependent Phosphoproteome.

FLP-U2OS cells expressing tetracycline inducible wild type or inhibitor resistant CK2 subunits were adapted in SILAC media. Exogenous CK2 was expressed by the addition of tetracycline for 48 hours followed by 4-hour treatment with CX-4945. Lysates were combined 1:1 and digested with Trypsin and Lys-C, followed by Phosphopeptide enrichment and analysis by LC-MS/MS. Relative quantitation was performed on raw mass spectra using MaxQuant. Identified and quantified phosphopeptides were analyzed using bioinformatics tools to investigate kinase-substrate relationships.

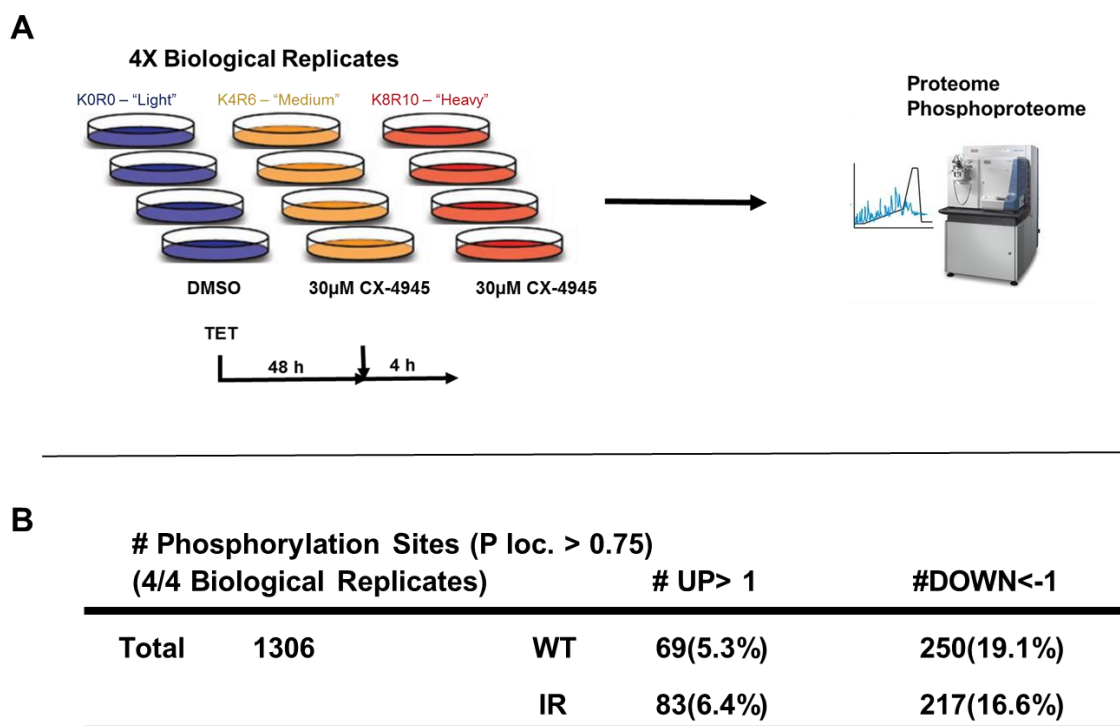


Figure 7. Experimental Layout and Data Summary

(A) Proteome and Phosphoproteome fractions were analyzed by LC-MS/MS in four biological replicates for both treated samples and controls (B) Number of identified phosphorylation sites quantified for all biological replicates and SILAC labels that changed in response to CX-4945 in wild type or inhibitor resistant CK2 mutant cell lines.

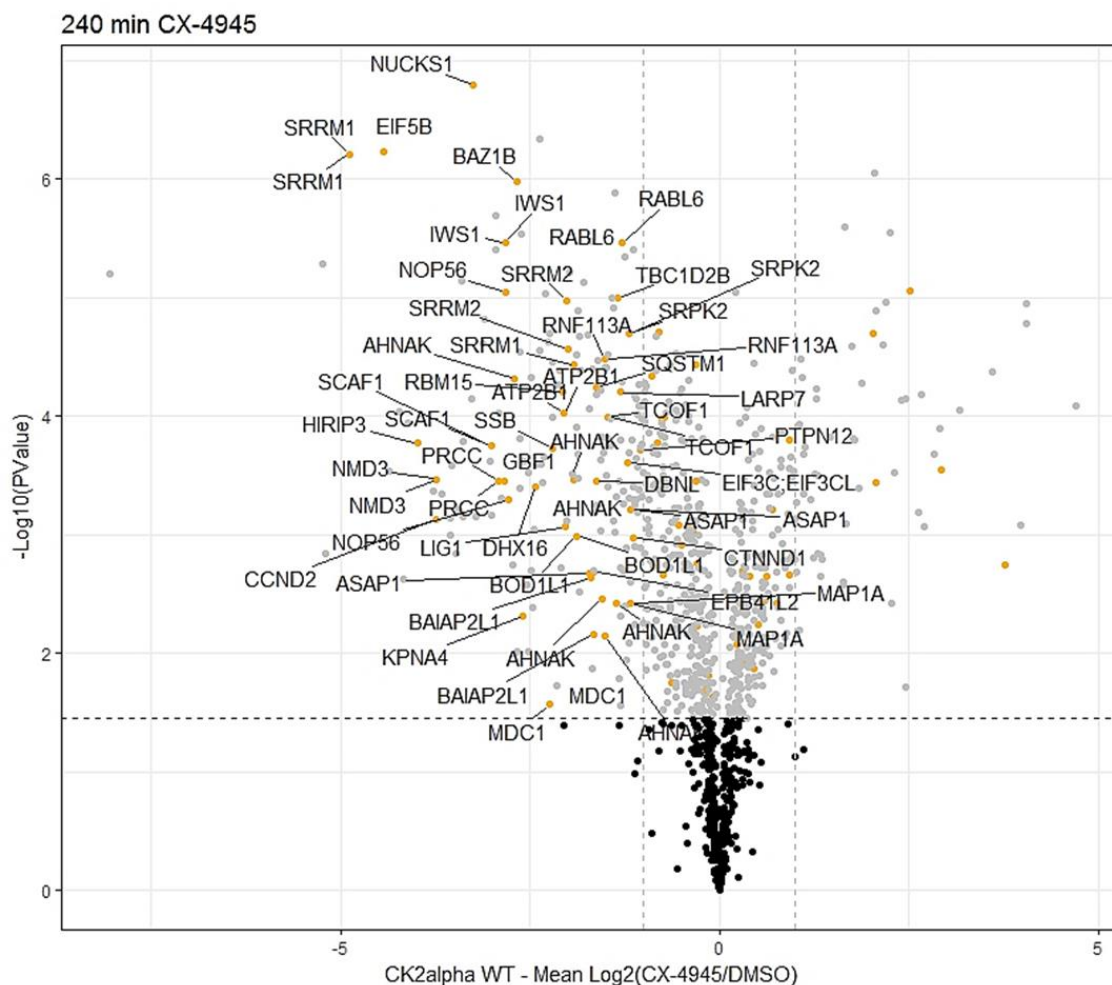


Figure 8. Volcano Plot of Quantified Phosphorylation sites from Inhibitor-Refractory U2OS cells treated with CX-4945. Quantified phosphorylation sites were tested for significance using a one-sample student's t-test with FDR corrections (<0.05). Points in grey exceeded statistical cutoff. Phosphorylation sites with at least a 25% recovery in the inhibitor resistant cell lines are highlighted in orange. Labelled sites exceed $\log_2 -1$ and are significant. Vertical dashed lines denote -1 and $+1 \log_2$ cutoffs; horizontal line denotes FDR threshold of 0.05

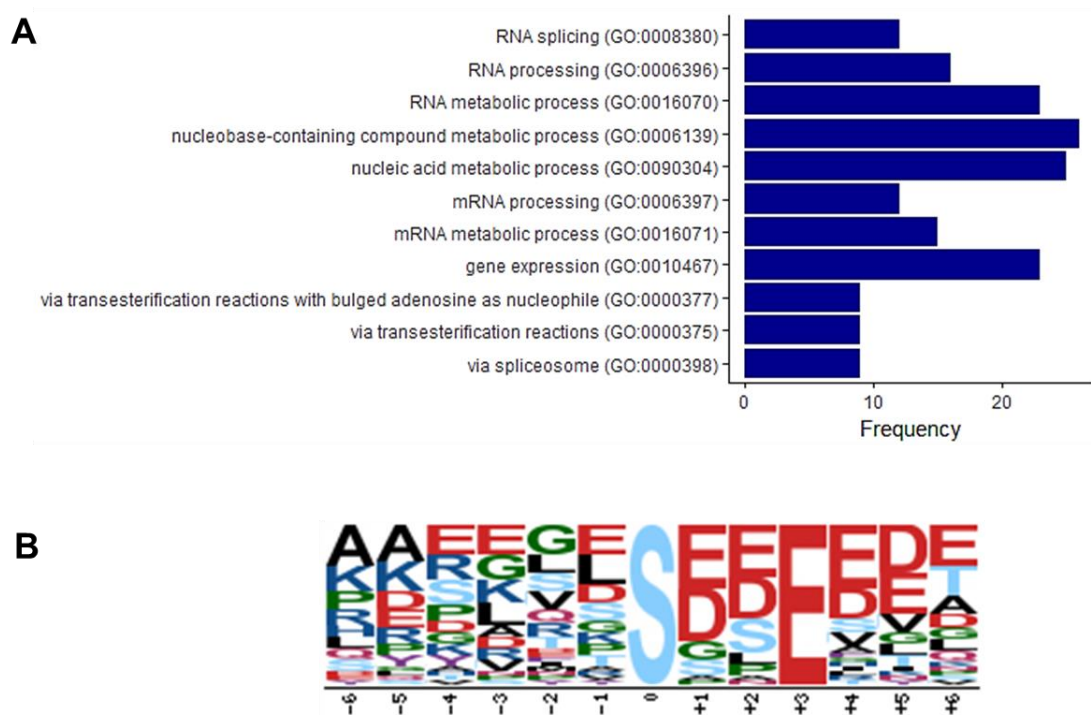


Figure 9. Analysis of Phosphorylation Sites Restored by Inhibitor Refractory CK2alpha. (A) Frequency of Gene Ontology terms associated with each of the recovered phosphorylation sites. GO terms represents biological function of associated protein group. (B) Analysis of recovered Phosphopeptides by Motif-X. Central residue is denoted by “S”.

3.4 Dynamic Changes in the Phosphoproteome are Independent of Protein Abundance

Changes in the proteome were monitored in parallel with the phosphoproteome by LC-MS/MS. The purpose of this is to ensure dynamic changes in the phosphoproteome result from perturbations in the kinase/phosphatase interplay at a particular phosphosite, and not from changes in the abundance of the parent protein. When observing the fold change distributions for the proteome, we can see that most quantified protein groups fall within the range of $\log_2 \pm 0.5$ (Supplementary Figure 7). This indicates that, in general, the proteome is not significantly changing as a result of CX-4945 treatment. Fold changes of phosphorylation sites that were determined to be statistically significant were plotted against the fold changes of their respective protein groups (Figure 10).

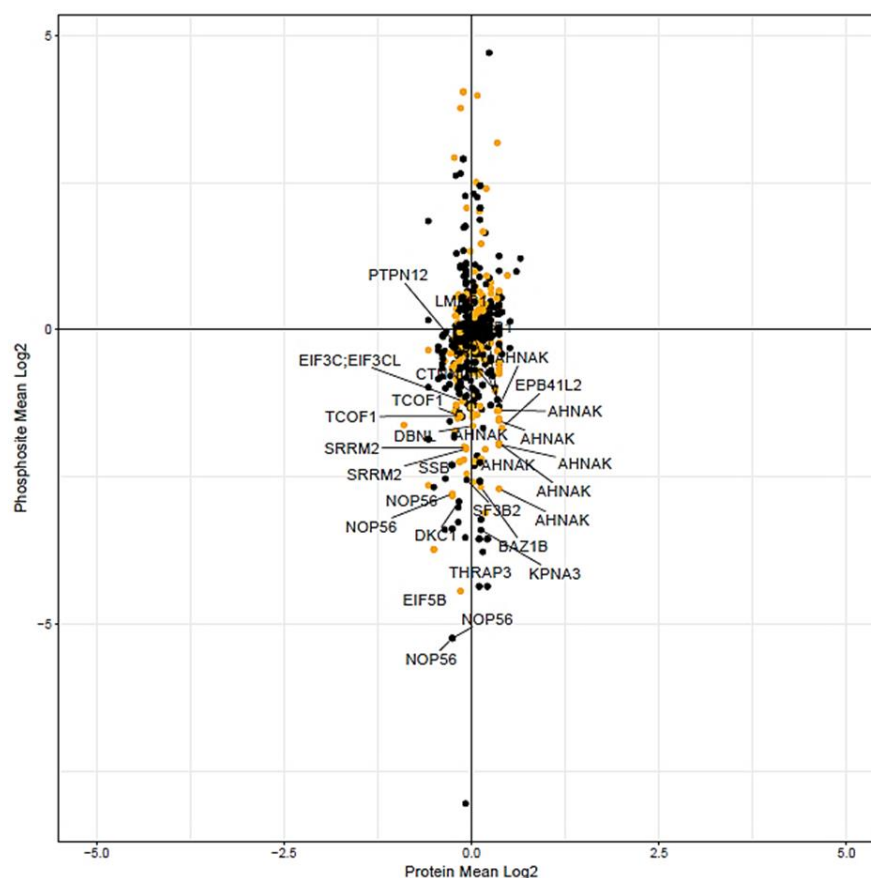


Figure 10. Comparison of Phosphorylation Site vs. Protein Abundance in Inhibitor Refractory U2OS cells treated with CX-4945. Identified phosphorylation sites that were statistically significant were plotted against their respective protein fold change ratio. The mean Log2 ratios for a phosphorylation site and the mean Log2 ratio for the respective protein group were displayed. All data was derived from 4 biological replicates. Phosphorylation sites labelled and highlighted in orange were recovered by at least 25% in the inhibitor resistant cells.

3.5 CX-4945 Treatment Modulates the Activity of Other Kinases

CK2 is known to regulate the activity of other kinases, either directly via phosphorylation, or indirectly mediating their activity via phosphorylation of cdc37 S13 (38). Furthermore, since CX-4945 is a small ATP competitive inhibitor, it is plausible that it may also target other kinases sharing similar structural properties with CK2. Given this information we sought out to determine the extent to which CX-4945 impacts other kinases. By comparing the wild-type and inhibitor resistant datasets, we hoped to distinguish the CK2 dependent and independent effects of inhibition by CX-4945. Accordingly, we employed the Kinase perturbation analysis (75). KinasePA uses a directional hypothesis testing framework to annotate and visualize kinases and their substrates that are perturbed by various combinatorial effects of treatments in phosphoproteomics experiments. In this case, the two conditions being compared are inhibitor resistant vs wild type. Unsurprisingly, the software demonstrates that CK2 is affected to the highest degree compared to other kinases that were affected. Interestingly, PKC and mTOR were also downregulated to a significant extent with reciprocal upregulation of the CDK kinase family and ERK1/2 (Figure 11). In addition to KinasePA, kinase-substrate enrichment analysis was performed using the PHOXTRACK software (76). The software infers the activation or inhibition of a particular kinase based on the trend of attributed phosphorylation sites. The analysis was largely consistent with that of KinasePA, in that substrates of mTOR decreased in phosphorylation, while substrates of CDK1 and ERK1/2 increased in phosphorylation. In particular, mTOR substrates RPTOR Ser859, and MAF1 Ser75 decreased in both the wild-type and

inhibitor refractory cell lines suggesting mTOR is a possible off-target of CX-4945 or that its activity may be regulated by CK2 such that it is impacted by inhibition of CK2.

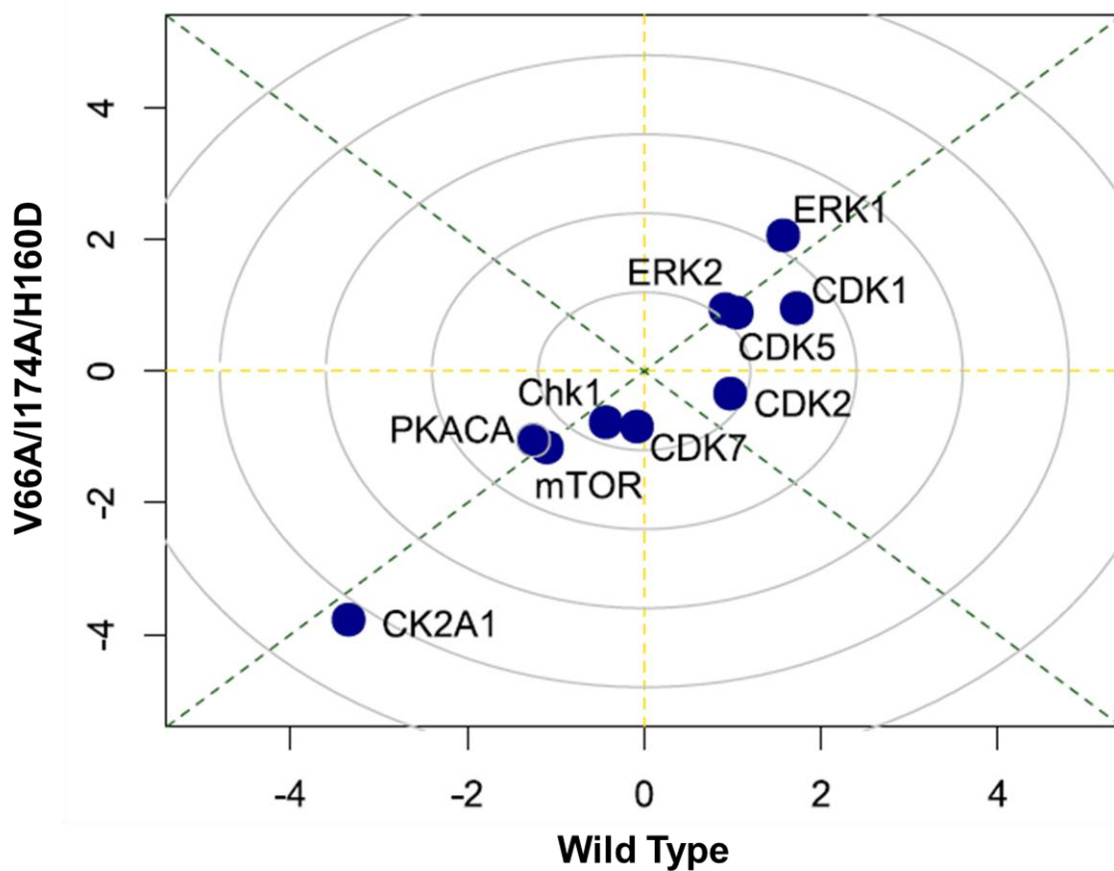


Figure 11. Kinase Perturbation Analysis Reveals Off-Targets of CX-4945.

The relationship between phosphoproteomic datasets obtained by treatment of wild-type and inhibitor refractory expressing U2OS cells with CX-4945 was analyzed using KinasePA. Distance from the origin indicates extent of kinase inhibition. Dashed lines represent slopes of -1 and +1. Kinases plotted along the line of +1 showed similar perturbation in both inhibitor resistant and wild type U2OS cells.

Table 1. Phosphorylation sites restored by inhibitor-refractory CK2-alpha in the presence of CX-4945. Phosphorylated proteins identified following CX-4945 treatment in Flp-U2OS cells expressing wild-type CK2-alpha were sorted based on their log2 fold changes, statistical significance, and whether phosphorylation was restored by the inhibitor-refractory CK2-alpha. Phosphorylation fold changes listed are in the wild-type (WT) or inhibitor-refractory (IR) U2OS cell lines in the presence of CX-4945. The IR/WT log2 ratio describes the changes in phosphorylation in the inhibitor-refractory cell line relative to the wild-type based on the heavy/medium isotope ratio.

Gene Name	Position	Fold Change log2(WT)	Fold Change log2(IR)	IR/WT Ratio (Log2)	Sequence	Networkin Prediction
EIF5B	S214	-4.444	-1.718	2.712	PGPNIESGNEDDD	CK2alpha
AHNAK	S5857	-1.37	0.788	2.122	SGVSLASKKSRLS	PKCBeta
IWS1	S398	-2.829	-0.954	1.784	RKAAVLSDSEDEE	CK2alpha
IWS1	S400	-2.829	-0.954	1.784	AAVLSDSEDEEKA	CK2alpha
ASAP1(1)	S717	-1.718	-0.36	1.389	QEEIDESDDDLDD	CK2alpha
AHNAK(1)	S5735	-1.95	-0.453	1.379	TGSPEASISGSKG	-
SRRM1	S874	-1.918	-0.606	1.305	PKKETESEAEEDNL	-
AHNAK(2)	S5735	-1.509	-0.192	1.261	TGSPEASISGSKG	-
EPB41L2	S87	-1.665	-0.466	1.209	WLKKQKSYTLVVA	CAMKIIalpha
AHNAK(1)	S5731	-1.928	-0.633	1.191	KGGVTGSPEASIS	-
AHNAK(2)	S5731	-1.548	-0.317	1.126	KGGVTGSPEASIS	-
ASAP1(2)	S717	-1.172	-0.148	1.061	QEEIDESDDDLDD	CK2alpha
ASAP1	S726	-1.172	-0.148	1.061	DLDDKPSPIKKER	-
DBNL	S269	-1.635	-0.621	1.053	QKERAMSTTSISS	-
PRCC	S157	-2.923	-2.029	1.017	ELHKGDSSEDEDE	-
PRCC	S159	-2.923	-2.029	1.017	HKGDSSEDEDEPT	-
CCND2	S271	-3.751	-3.078	0.942	QRDGSKSEDELDQ	CDK6
NUCKS1	S19	-3.248	-2.356	0.918	YSQFQESDDADE	-
AHNAK	S5841	-2.704	-1.772	0.9	HYEVTGSDDDETGK	-
GBF1	S1318	-2.844	-1.931	0.894	LDRGYTSDSEVYT	CK2alpha
DHX16	S103	-2.431	-1.576	0.862	YRLLEDSEESSEE	-
RABL6	S596	-1.287	-0.333	0.857	PVRDDPSDVTDED	-
RABL6	T599	-1.287	-0.333	0.857	DDPSDVTDEDEGP	-
EIF3C	S39	-1.21	-0.395	0.797	KQPLLLSEDEEDT	CK2alpha
HIRIP3	S227	-3.993	-3.186	0.786	KESEQESEEEILA	-
NOP56	S519	-2.826	-1.999	0.784	SKEELMSSDLEET	-
RNF113A	S84	-1.52	-0.718	0.752	AAYGDLSSEEEEEE	-
RNF113A	S85	-1.52	-0.718	0.752	AYGDLSSEEEEEN	-
NOP56	S520	-2.788	-2.025	0.73	KEELMSSDLEETA	CK2alpha
CTNND1	S167	-1.133	-0.396	0.725	QVRVGGSSVDLHR	-

TBC1D2B	S957	-1.343	-0.606	0.721	DKGELVSDEEEDT	-
SSB	S366	-2.21	-1.479	0.709	KKTKFASDDEHDE	CK2alpha
SRRM1	S874	-4.887	-4.252	0.683	PKKETESEAEDNL	-
SRRM1	T872	-4.887	-4.252	0.683	PEPKKETESEAED	-
TCOF1	S1299	-1.47	-0.769	0.629	GEGGEASVSPEKT	CK2A2
TCOF1	S1301	-1.47	-0.769	0.629	GGEASVSPEKTST	PKCalpha
SCAF1	S734	-3.016	-2.232	0.623	REVLVDSEGLSGE	-
SCAF1	S738	-3.016	-2.232	0.623	YDSEGLSGEERGG	-
SRPK2	S494	-1.191	-0.591	0.604	DRSRTVSASSTGD	-
SRPK2	T498	-1.191	-0.591	0.604	TVSASSTGDLPKA	PKCBeta
PTPN12	S305	-1.04	-0.443	0.576	KLERNLSFEIKKV	-
MAP1A	S526	-1.176	-0.628	0.575	HRELVLSSPEDLT	-
MAP1A	S527	-1.176	-0.628	0.575	RELVLSSPEDLTQ	-
RBM15	S250	-2.068	-1.547	0.565	GGQRSLSPGGAAL	-
BAZ1B	S1464	-2.672	-2.078	0.555	AEDEGDSEPEAVG	-
SRRM2	S875	-2.027	-1.468	0.551	RRSCFESSPDPEL	-
SRRM2	S876	-2.007	-1.448	0.51	RSCFESSPDPELK	-
LARP7	S258	-1.315	-0.708	0.506	KRSRPTSEGSIDIE	-

4 Discussion

Protein Kinase CK2 expression is deregulated in a variety of human cancers, as evidenced by a recent publication documenting CK2 mRNA expression data in the Oncomine data base (40). CK2 over-expression, as well as its mechanistic role in tumorigenesis and maintenance of the multi-drug resistant phenotype have promoted its emerge as a promising therapeutic target. CX-4945 is the first clinical-stage, orally available small molecule ATP competitive inhibitor of CK2. Although the compound has begun to show clinical promise, questions regarding the specificity of CX-4945 and its proclivity to target other kinases remain unanswered. In addition, the majority of phosphoproteomic investigations of CK2 employ small-molecule compounds designed to inhibit CK2 that have not been fully characterized in cells. Therefore, we sought to use phosphoproteomics in combination with inhibitor refractory cell lines to identify reliable biomarkers of CK2 activity and to investigate the divergent (CK2 independent) effects of CX-4945 treatment, as well as further our understanding of CK2's role in cellular signalling pathways.

Characterization of Inhibitor Refractory Flp-U2OS Cell Lines

Initial profiling of the inhibitor refractory and wild-type Flp-U2OS cell lines was performed to assess the extent to which the exogenously expressed CK2 α subunits are being incorporated into the existing cellular machinery. We first sought to determine the extent to which the engineered cell lines are capable of over-expressing the inhibitor

refractory and wild-type subunits. Prolonged induction and monitoring of the induced exogenous proteins for a period of 5 days, followed by western blot analysis using anti-CK2alpha/alpha' antibodies demonstrated that we could achieve roughly equal level of expression between that of the exogenous and endogenous CK2alpha. Interestingly, over the 5 days there was a significant reduction in the levels of CK2alpha'. This raises the question of whether or not there exists a threshold in the cellular level of CK2. Given that elevated levels of CK2 have been documented in many cancers, it is possible that perturbations in gene expression occurring in malignancies could override this threshold leading to its elevated expression.

CK2 substrates can be classified based on whether they are phosphorylated by the holoenzyme complex or by the free catalytic subunits (86). Therefore, the careful interpretation of our phosphoproteomic analysis must take into account whether or not the exogenously expressed inhibitor refractory and wild-type subunits are capable of forming complexes with the endogenously expressed regulatory CK2beta subunit. Immunoprecipitation assays where exogenous CK2beta was isolated from protein lysates showed that it was accompanied by the exogenously expressed subunits, suggesting that complex formation does indeed occur following expression. In addition to forming complexes, it also appears that the subunits are also catalytically active when in the complex formation. The auto-phosphorylation of CK2beta on site Ser2 occurs as a result of complex formation with the catalytic subunits (83). Preliminary time-course experiments with CX-4945 demonstrated using a phospho-specific antibody for CK2beta that upon treatment, the inhibitor refractory cell line was able to restore phosphorylation of the auto-phosphorylation sites (Supplemental Figure 1). This provides further evidence

of the exogenously expressed proteins being incorporated into the holoenzyme subunit, and additionally demonstrates that the inhibitor refractory mutant is functional when in complex. Although we have confirmation that the exogenously expressed subunits form complexes with CK2beta, we cannot be sure of the exact stoichiometry of the interaction. This is consistent with previous investigations of exogenously expressed CK2-Beta that was found to form complexes with the endogenous CK2 catalytic subunits (82). Given that the exogenously expressed subunits make up close to half of the total pool of catalytic CK2, there is a possibility that the exogenous CK2beta preferentially forms complexes with endogenous CK2alpha.

Following characterization of the engineered cell lines, we then sought to identify time points suitable for phosphoproteomic profiling in the presence of CX-4945. Prolonged periods of sustained exogenous CK2 expression revealed that after 48 hours in the presence of tetracycline, levels of exogenous CK2alpha (inhibitor refractory and wild-type) began to plateau and reach a “steady state”. Time courses with various concentrations of CX-4945 have previously identified 30 μ M as a concentration used for treatment that results in a high extent of CK2 inhibition while not being in excess (Figure 5). In order to maintain consistency with previous phosphoproteomic analysis of CX-4945, we chose the 4 hour time point. Initial assays determined that this time point precedes the activation of apoptotic pathways, which could potentially confound the phosphoproteomic analysis as it would be impossible to distinguish apoptotic signalling events from bona-fide CK2-dependent signalling. Initial experiments with the inhibitor refractory and wild-type cell lines demonstrated that the inhibitor resistant cell line was capable of restoring phosphorylation, as indicated by western blotting with the phospho-

specific antibody for the bona-fide CK2 substrate EI2FS2 after treatment with 30uM CX-4945 for 4 hours.

Phosphoproteomic Investigation of CK2 Using Inhibitor Refractory Cell lines

The phosphoproteomic analysis of CK2 using CX-4945 and inhibitor refractory cell lines resulted in a dataset that demonstrates the utility of our approach for the discovery of CK2 activity biomarkers and CX-4945 off-targets. However, when using small molecule compounds to inhibit the activity of kinases for downstream phosphoproteomic analysis there are a few key points that must be taken into consideration. There is a common misconception that once a kinase has been inhibited in a cell, its substrates will immediately become dephosphorylated. This can be true of kinases that are inactive under basal conditions which are only activated in response to specific stimuli, but it is not always the case for constitutively active kinases such as CK2. Given that CK2 is a constitutively active kinase and under basal conditions ensures substantial phosphorylation of its targets, differential phosphatase activity is required to regulate the phosphorylation status of its substrates. Therefore, when inhibiting CK2 with a small-molecule compound such as CX-4945 we would not expect a uniform decrease in phosphorylation among all CK2 substrates. Rather, we would expect that the extent of dephosphorylation among CK2 substrates is reflective of the activity of their putative protein phosphatases. It is also important to note that residues embedded within acidic sequences (such as those phosphorylated by CK2) typically display much slower turnover than those in proximity to neutral/basic residues (87). Using phospho-specific antibodies against bona-fide CK2 substrates, we validated that CK2 activity is drastically diminished after 4 hours of treatment with CX-4945. However, this is not guaranteed to be reflected

in the phosphorylation status of all of CK2's substrates at such a short time point. Instead, it is likely that sites that are targets of highly active phosphatases will show greater dephosphorylation than those whose putative phosphatases are not as active. This will have implications for the ability of the inhibitor refractory mutant to restore phosphorylation of a given phosphorylation site. Given that the ability of the inhibitor refractory mutant to restore phosphorylation of CK2 substrates has been demonstrated, we would expect that the phosphoproteomic dataset of the inhibitor refractory cell line show phosphosites whose phosphorylation is reduced to a lesser extent than the same site in the wild-type cell line. However, the ability of the inhibitor refractory mutant will greatly depend on phosphatase activity and the cellular context of a given phosphosite. These aspects need to be taken into consideration when using this approach for the identification of CK2 biomarkers and inhibitor off-targets.

Phosphoproteomic analysis of the inhibitor refractory cell line revealed a significant number of phosphosites whose phosphorylation was restored compared to the wild-type cell line. Of the 250 quantified phosphorylation sites in the wild-type cell line that had a log₂ fold change less than -1, 48 of them were recovered by the inhibitor refractory mutant by at least 25% and are classified as CK2 dependent. Of note is EIF5B Ser214, which had a 6.55-fold recovery in phosphorylation in the inhibitor refractory cell line versus the wild-type. Given the robust recovery in phosphorylation by the inhibitor refractory mutant, it is likely that this is a substrate of CK2 and is a prime candidate to serve as a CK2 activity biomarker. This site has not been documented in the literature as CK2 dependent, however, it fits the specificity determinants for CK2 and is identified as a potential CK2 substrate by KinomeXplorer. Previous studies have documented this site

and have attributed its phosphorylation to be mTOR dependent. In a phosphoproteomic analysis of the mTOR inhibitor rapamycin, Jian et al (2016) found the Ser214 site on EIF5B was drastically reduced in phosphorylation as a result of mTOR inhibition (88). Using a phospho-mimetic and Ser214Ala mutants, it was discovered that this site is responsible for EIF5B's interaction with NAT10, an RNA acetyltransferase responsible for 18S rRNA processing. EIF5B is itself responsible for the joining of 60S subunits with the pre-40S subunits and plays a significant role in translational initiation (89). Along with CK2's phosphorylation of EIF2S2, this further emphasizes CK2's role in protein synthesis. There are other reported instances of CK2 and mTOR phosphorylating overlapping proteins. It has been reported that both mTOR and CK2 phosphorylate EIF2S2 on Ser2 and Ser67 (90) to stimulate the assembly of the eIF4F complex, a rate limiting step in translation initiation regulated by eIF2 α phosphorylation and the mTOR/4E-BP pathway (91). Taken together with our findings, it is plausible that CK2 and mTOR work in concert to regulate protein synthesis via translational initiation. Given the close proximity of phospho-acceptor residues known to be phosphorylated with both CK2 and mTOR, it is possible that phosphorylation of a site by mTOR may serve as priming for phosphorylation by mTOR and vice-versa.

Analysis of quantified phosphorylation sites that changed in response to CX-4945 treatment in the wild-type cell line revealed several known CK2 substrates that showed varying levels of reduced phosphorylation to a greater extent than EIF2S2. This is consistent with the phosphoproteomic analysis of Rabalski (2017) (85). Among these sites are TOP2A Ser1377, a well-documented CK2 substrate that showed an 8-fold decrease compared to the DMSO vehicle treatment (92). In addition another documented

CK2 substrate SSB which is phosphorylated by CK2 on Ser366 (93) showed a decrease of Ser366 phosphorylation of approximately 4.5-fold compared to the vehicle DMSO treatment. Given the high extent of dephosphorylation of known CK2 substrates it's clear that its inhibition was achieved. However, previous studies with other CK2 inhibitors have shown that 3 hour of CK2 inhibition may not be sufficient to result in decreased phosphorylation of the majority of its substrates (94). Additionally, many CK2 phosphorylation sites that were downregulated significantly were not restored to a significant degree in the inhibitor refractory cell line. Although it is clear CK2 inhibition was achieved as indicated by the decreased phosphorylation of known substrates, the extent to which they were dephosphorylated varies quite dramatically between them. As previously mentioned, there are several reasons why this could be. Aside from the differential activity of protein phosphatases, it is possible that at the 4-hour time point, there is not sufficient quantities of the inhibitor refractory mutant available to restore phosphorylation of those particular CK2 substrates. Given that the inhibitor refractory mutants can only be expressed at a level that is equivalent to that of the endogenous, the system will always be comprised of 50% inhibitor refractory and 50% wild-type. The restoration of phosphorylation by the inhibitor refractory subunit will greatly depend on the composition of local pools of CK2. If at a given sub-cellular location there is higher amounts of inhibitor refractory CK2alpha compared to the wild-type, only then would we expect to see a drastic increase in phosphorylation in the presence of CX-4945. EIF2S2 Ser2 has also been characterized as a CK2beta dependent phosphorylation site. It is therefore possible that the holoenzyme complex containing the inhibitor refractory CK2alpha was not present in sufficient quantities to restore phosphorylation at that site.

It is also interesting to note that phosphorylation of some CK2 substrates increase in response to CX-4945 treatment. This could be due to a decrease in abundance of a multiply-phosphorylated peptide, which would increase the stoichiometry of the corresponding singly or doubly phosphorylated peptide at a different phospho-acceptor residue on the peptide. This trend has been documented in other phosphoproteomics analysis with the CK2 inhibitor Quinalizarin (94). Another possibility is that the close proximity of phospho-acceptor residues can themselves serve as specificity determinants for hierarchical phosphorylation by CK2 (95), such that their dephosphorylation results in an apparent increase in the phosphopeptide containing the CK2 phosphorylation site. Phosphorylation sites that demonstrate large changes as a result of CK2 inhibition could serve as useful indicators of CK2 activity in cells as well as provide insight into the pathways regulated by CK2. However, with ATP-competitive inhibitors such as CX-4945, we must be mindful of off-targets effects confounding the analysis. In this respect, the inhibitor refractory mutant should shed light on which processes and phosphorylation sites are dependent on CK2 activity.

Analysis of CX-4945 Treatment on the Activity of Other Kinases.

Treatment with CX-4945 resulted in a dynamic phosphoproteome, with a significant number of phosphorylation sites belonging to other kinases decreasing in both the inhibitor refractory and wild type cell lines. CK2 is well known to regulate the activity of other kinases via either direct phosphorylation, or through its phosphorylation of Hsp90 co-chaperone cdc37 on Ser13 (37). Although cdc37 Ser13 was not quantified in this phosphoproteomic analysis, previous experiments have demonstrated that this site is not significantly downregulated in response to 4 hour CX-4945 treatment (85). Therefore, it

is likely that the responses associated with other kinases results from direct manipulation by CX-4945. Of note, there were several substrates of mTOR that were significantly dephosphorylated. In particular, Raptor Ser859 and Ser863 were downregulated in both wild-type and inhibitor refractory cell lines. These sites have a known role in the activation of mTOR and downstream signaling, demonstrated by the fact that Ser863 mutants of Raptor reduced activity of downstream kinases (96). Similarly, MAF1 Ser75, a known substrate of mTOR is significantly decreased, and is known to play a role in the control of RNA polymerase III-dependent transcription in cancer cells (97). Previous phosphoproteomic analysis of CX-4945 have also demonstrated that upon treatment, there is a significant decrease in phosphorylation of mTOR substrates (85). In addition, it has been observed that CX-4945 treatment induces autophagy, a process well known to be regulated by mTOR (98). In vitro analysis of CX-4945 in pre-clinical studies showed that its IC₅₀ values were significantly higher for mTOR than for CK2 (99). These findings raise serious questions regarding the specificity of CX-4945 in a cellular context.

Phosphorylation sites that showed an increase in response to CX-4945 treatment were attributed to ERK1 and CDK1 kinases. A similar response was seen in Rabalski (2017) who saw an increase in CDK1/CDK2 substrates as a result of CX-4945 treatment in HeLa cells. CK2 has been found to phosphorylate cyclin-H, the activating cyclin of CDK7(100). CDK7 is the catalytic subunit of the CDK-activating (CAK) enzymatic complex which is responsible for activating CDK's 1, 2 and 4(101). Given that CK2 has an activating role in CDK activity, it is interesting that CK2 inhibition by CX-4945 results in the activation of CDK's rather than their inhibition. CX-4945 treatment also resulted in the increased phosphorylation of several ERK1/2 substrates. This presents an

interesting situation, given that CK2 is a pro-survival kinase, and ERK signalling is usually associated with cell growth and proliferation (102). CK2 is known to have a regulatory association with ERK. Through phosphorylation of ERK's nuclear translocation signal (NTS), CK2 regulates the nuclear translocation of activated ERK by phosphorylation Ser246 and Ser244 allowing it to bind Importin7 (103). CK2alpha has also been implicated in regulating the ERK-specific phosphatase cdc25B (104). Given that CDK1 and ERK1 activity is shown to increase upon CX-4945 treatment, it is possible that alternative pathway activating either as a result of direct CK2 inhibition or CX-4945 off-targets are the causal factor.

Conclusions

The reversible phosphorylation of proteins is a critical post-translational modifications responsible for the tight regulation of essential cellular processes. Given its involvement in a number of vital pathways as well as its deregulation in many cancers, CK2 has garnered attention as a therapeutic target. This has led to the development of therapeutic compounds designed to inhibit CK2. In particular, the ATP-competitive CX-4945 has shown the most promise and is currently in the clinical regulatory pipeline. CX-4945 has been used widely in the literature to investigate the specific cellular signalling events mediated by CK2. However, these investigations often study one particular pathway in isolation and do not consider the potential effects of CX-4945 treatment on other pathways. In this respect, these investigations provide anecdotal evidence for CK2 involvement in a particular pathway of interest. The shared structural similarities between protein kinases presents a challenge in designing highly specific small molecular inhibitors and is thus a significant limitation for their use in biological experiments.

Therefore we have developed strategies to validate inhibitor engagement with CK2. In this investigation, we were able to optimize a phosphoproteomic and chemical genetic workflow to identify CK2-dependent phosphorylation sites and analyze the specificity of clinical stage CK2 inhibitor CX-4945. This studies has enabled the identification of novel biological substrates of CK2, and in parallel has uncovered potential off-target effects of CX-4945. These novel phosphorylation sites have the potential to be used as clinical biomarkers of CK2 activity. In theory, these biomarkers could be used as a readout of CK2 activity in clinical samples, which could help to inform whether or not CK2 targeted therapeutics would be beneficial for an individual's treatment. These sites will also be of value in validating newly developed inhibitors of CK2, given that their dephosphorylation will be indicative of CK2 inhibition. This study has also uncovered effects due to CX-4945 treatment that are not the result of CK2 inhibition. These findings raise speculation as to the precise cellular mechanism by which CX-4945 operates. More broadly, this investigation emphasizes the need for rigorous evaluation of newly developed kinase inhibitors using unbiased methods on a global scale. Given the mounting evidence for ATP-competitive inhibitors regulating kinases other than their intended targets, we can no longer rely solely on in-vitro analysis using recombinant kinases to evaluate their specificity

Future Directions

The use of cell lines engineered to harbour the inhibitor refractory CK2 α subunit has been demonstrated here. However, there are several aspects of the system that could be improved upon in order to remove as many confounding factors as possible for their use in proteomic investigations. We were able to achieve a system in which

approximately half of the cellular pool of CK2 was made up of the inhibitor refractory mutant. The next logical step in improving this system would be to devise a strategy to remove all of the endogenous CK2 α , such that the entire pool of catalytic CK2 α is made up of the inhibitor refractory mutant. A potential way that this could be done is by using the CRISPR-Cas9 system to knock-out endogenous CK2 α . Given that CK2 catalytic subunits are essential for cell viability, knocking it out could prove challenging. Since the expression of the inhibitor resistant subunits are inducible by the addition of tetracycline, it is possible that we could knockout the endogenous subunits while maintaining sufficient levels of CK2 α to keep the cells viable.

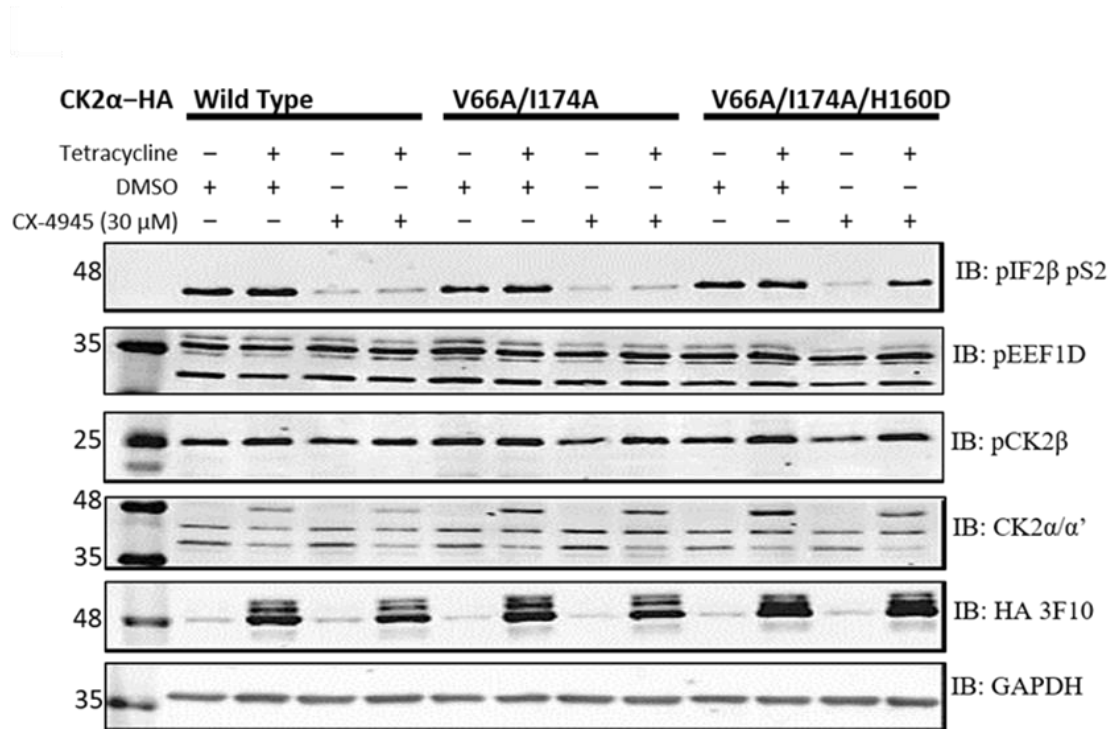
Although the 4 hour treatment with CX-4945 resulted in dynamic changes to the phosphoproteome, it is still a relatively short period of exposure when compared to the compounds use in clinical settings. Therefore, it would be beneficial to repeat the experiment with the inhibitor refractory mutant with longer periods of exposure to CX-4945. Investigating longer time points of 8, 24, and 48 hours would perhaps uncover phosphorylation sites that are rescued by the inhibitor refractory mutant, but are not dynamic enough to be seen at the 4 hour time point used in this investigation. Not only would this be beneficial in discovering novel substrates of CK2 that are less dynamic, but the increased exposure to CX-4945 would allow the compound time to bind other kinases that may have affinity for it. Thus the longer exposure time could be of service in gauging the extent to which CX-4945 binds off-targets, and allow for a more precise analysis since more phosphorylation sites should show higher fold changes. It would also be beneficial to repeat a similar investigation using another CK2 inhibitor with different structural properties to that of CX-4945. In particular, the CK2 inhibitor VIII compound

has shown promise as a highly potent inhibitor of CK2 in preliminary assays and is also unable to inhibit the inhibitor refractory CK2alpha mutants. Given that CX-4945 and Inhibitor VIII are completely unrelated structures, a phosphoproteomic analysis using each of these could help in distinguishing cellular processes that are CK2-dependent. The two compounds would likely have very different off-targets in cells, therefore only those phosphorylation sites that are down-regulated and restored by the inhibitor refractory mutant after treatment with both inhibitors could be considered CK2-dependent, providing an additional measure of validation.

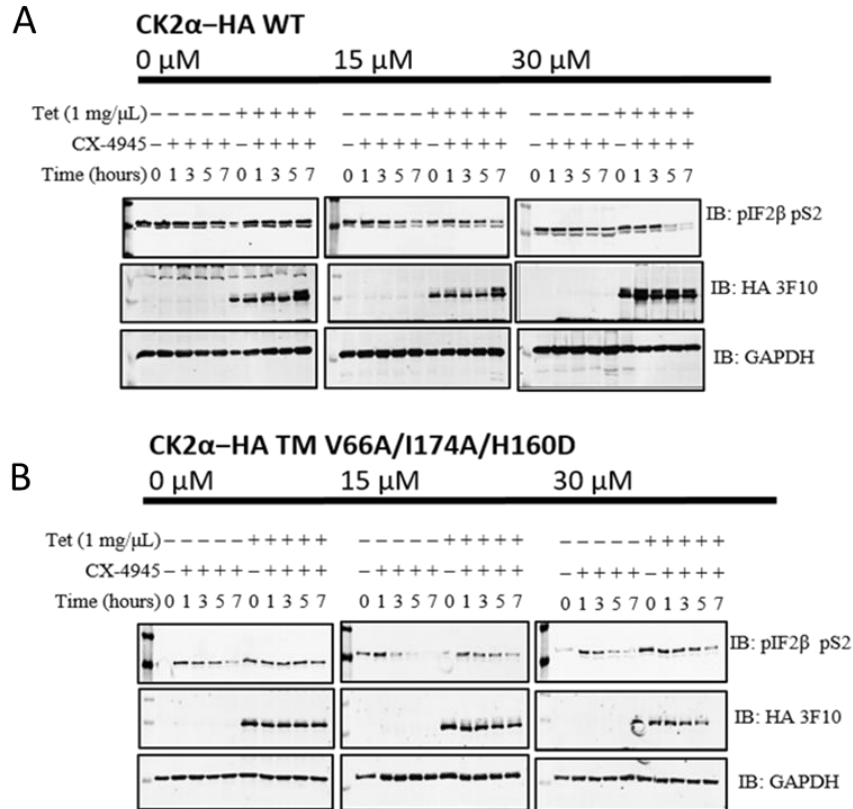
One limitation in using engineered cell lines harbouring inhibitor refractory mutants of the CK2alpha subunit only is that it cannot distinguish between phosphorylation sites that are solely dependent on phosphorylation by CK2alpha'. Given that there is evidence of substrates that are preferentially phosphorylated by one of the two catalytic isoforms, a comparative analysis of inhibitor refractory CK2alpha and CK2alpha' could help uncover isoform specific substrates. For this investigation to be undertaken, a cell line expressing the inhibitor refractory mutant of CK2alpha' would need to be developed. This has posed a challenge, since the exogenous expression of CK2alpha' has not matched the levels achieved with CK2alpha. To extend this further would be to repeat the same analysis using cell lines which express the inhibitor refractory forms of the catalytic subunits with simultaneous expression of the CK2beta regulatory subunit. There have been many documented cases of CK2 substrates that are preferentially phosphorylated by the holo-enzyme and the catalytic subunits on their own. The Flp-in Trex system, with manipulation using cDNA containing internal ribosome binding sites would be used for this type of analysis.

The identification of phosphorylation sites that are dynamically down regulated as a result of CX-4945 treatment and that are sufficiently restored by the inhibitor refractory mutant cell line have provided a panel of candidate activity biomarkers upon which the actions of CX-4945 and other CK2 inhibitors can be monitored in various cell lines. Given that the phosphorylation sites in this investigation were derived from peptides that were detected using data-dependent acquisition methods, there is a high likelihood of successfully deriving a targeted mass-spectrometry assay to profile CK2 activity. Selected reaction monitoring (SRM) is the most often used method of profiling proteotypic peptides and is considered the gold standard. Advances in the development of proteomic instrumentation have allowed for a similar technique known as parallel reaction monitoring (PRM) which can be performed using hybrid instruments containing both orbitrap and quadrupole mass analyzers. This approach is advantageous because of its ability to simultaneously monitor all fragment ions from a precursor ion selected in MS1 analysis and does not require prior optimization of precursor and fragment ion transitions. For these studies, candidate phosphopeptides that were identified in this and previous studies can be synthesized and used as internal standards that can be “spiked” into tryptic digests of cells treated with various CK2 inhibitors. This approach could be used to study the activity of CK2 in a variety of cellular contexts. For example, synthetic isotopically labelled peptides that are representative of CK2 activity could be used to monitor its activity in various biological contexts. Given CK2’s therapeutic potential, these candidate biomarkers could also be used to monitor its activity in clinical samples derived from patient tissues.

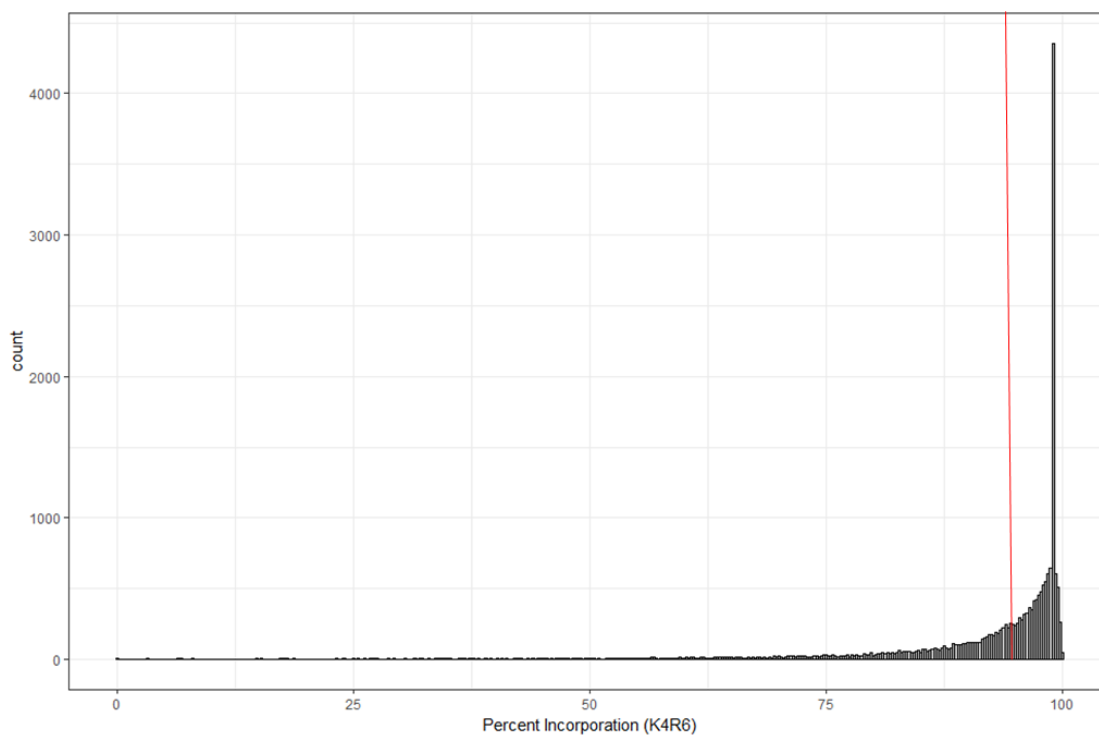
5 Supplemental Figures



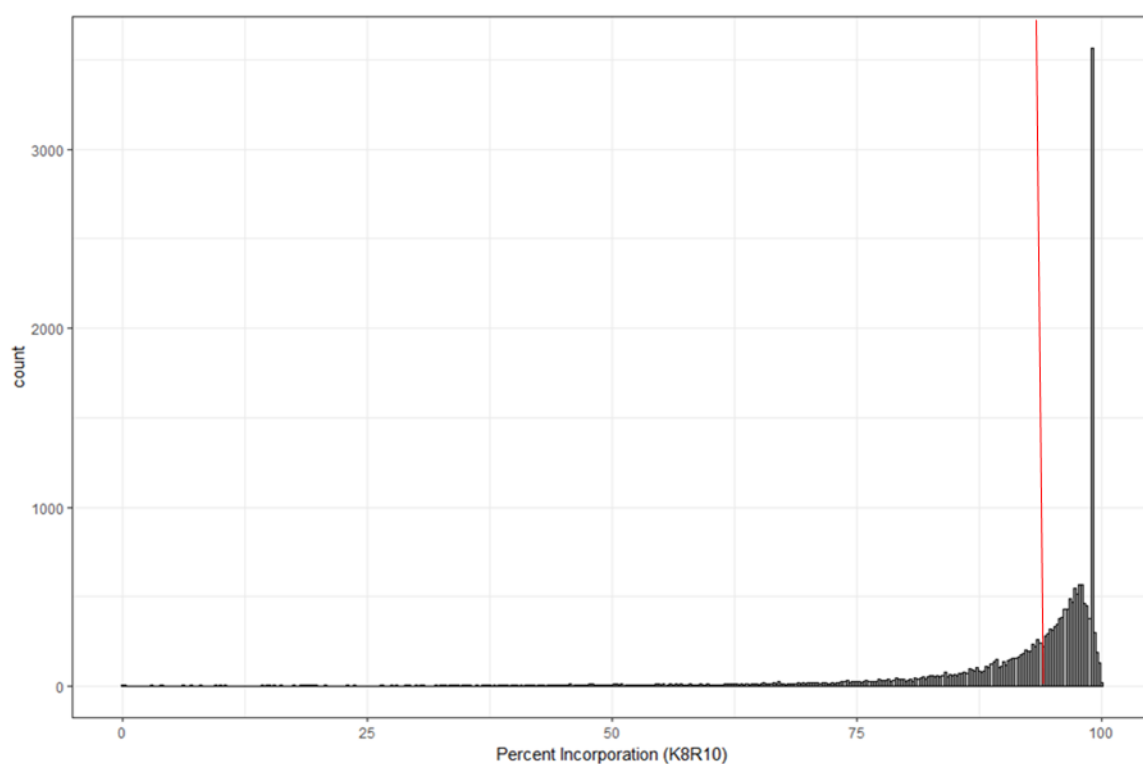
12. (Supplemental Figure 1). Measuring the ability of CK2-alpha mutants to overcome the inhibition of CX-4945. Cells were induced for 48 hours with 1 μg/ml tetracycline prior to treatment with 30 μM CX-4945 for 7 hours. Cells were harvested, lysate was collected and separated by SDS-PAGE prior to western blotting with pEEF1D, pCK2β and pIF2β (pEIF2S2) antibodies to measure the recovery of the inhibitor-refractory mutants in the presence of the inhibitor.



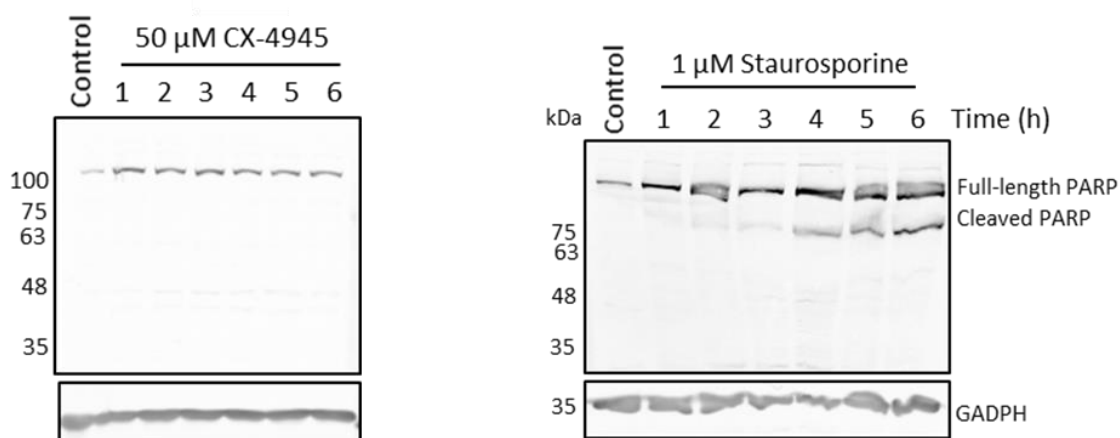
13. (Supplemental Figure 2). Optimal CX-4945 concentration for the inhibition of CK2 in U2OS cells expressing wild-type and inhibitor refractory (V66A/I174A/H160D) CK2-alpha. Expression of CK2-alpha was induced in Flp-In U2OS cells for 48 hours with 1 μ g/ml tetracycline, then treated with various concentrations of CX-4945 at various time points. Protein lysate was harvested and blotted and incubated with pIF2 β antibody to measure the recovery of the inhibitor-refractory mutants in the presence of inhibitor.



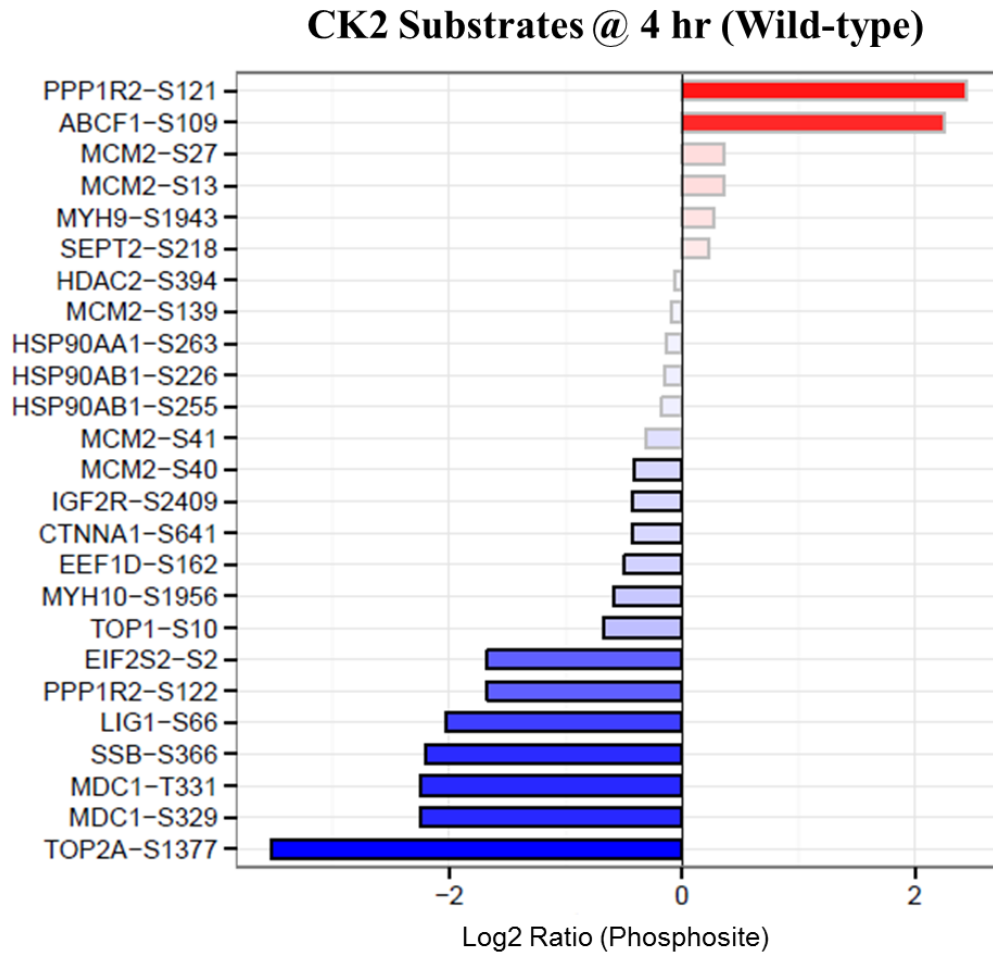
14. (Supplemental Figure 3). Frequency Distribution of SILAC Medium Labelled Arginine and Lysine Incorporated Peptides. Flp-U2OS cells were adapted in silac medium over 8 days. An aliquot of medium labelled cells was harvested and processed as described in the materials and methods section. Distribution is representative of all lysine and arginine peptides that were quantified. Median incorporation was calculated to be 96.6%. Red vertical line indicates 95% incorporation.



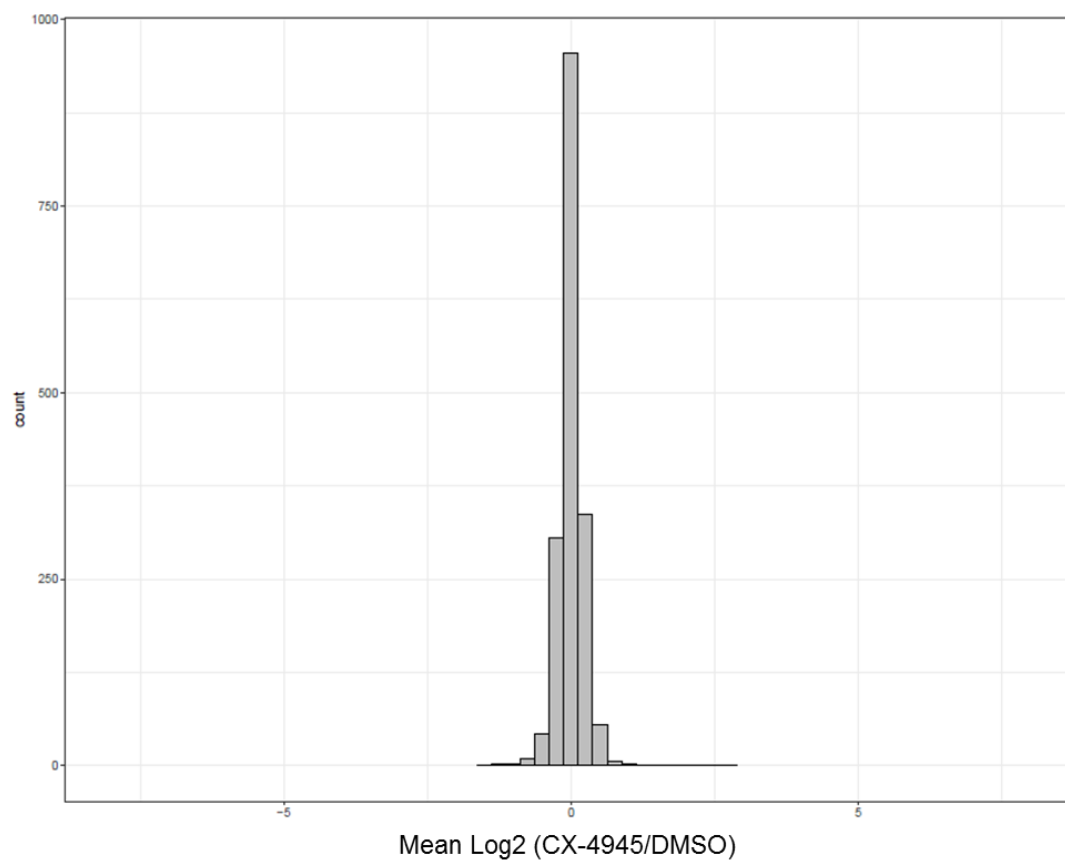
15 (Supplemental Figure 4). Frequency Distribution of Heavy Labelled SILAC Arginine and Lysine Incorporated Peptides. Flp-U2OS cells were adapted in silac medium over 8 days. An aliquot of heavy labelled cells was harvested and processed as described in the materials and methods section. Distribution is representative of all lysine and arginine peptides that were quantified. Median incorporation was calculated to be 95.6%. Red vertical line indicates 95% incorporation.



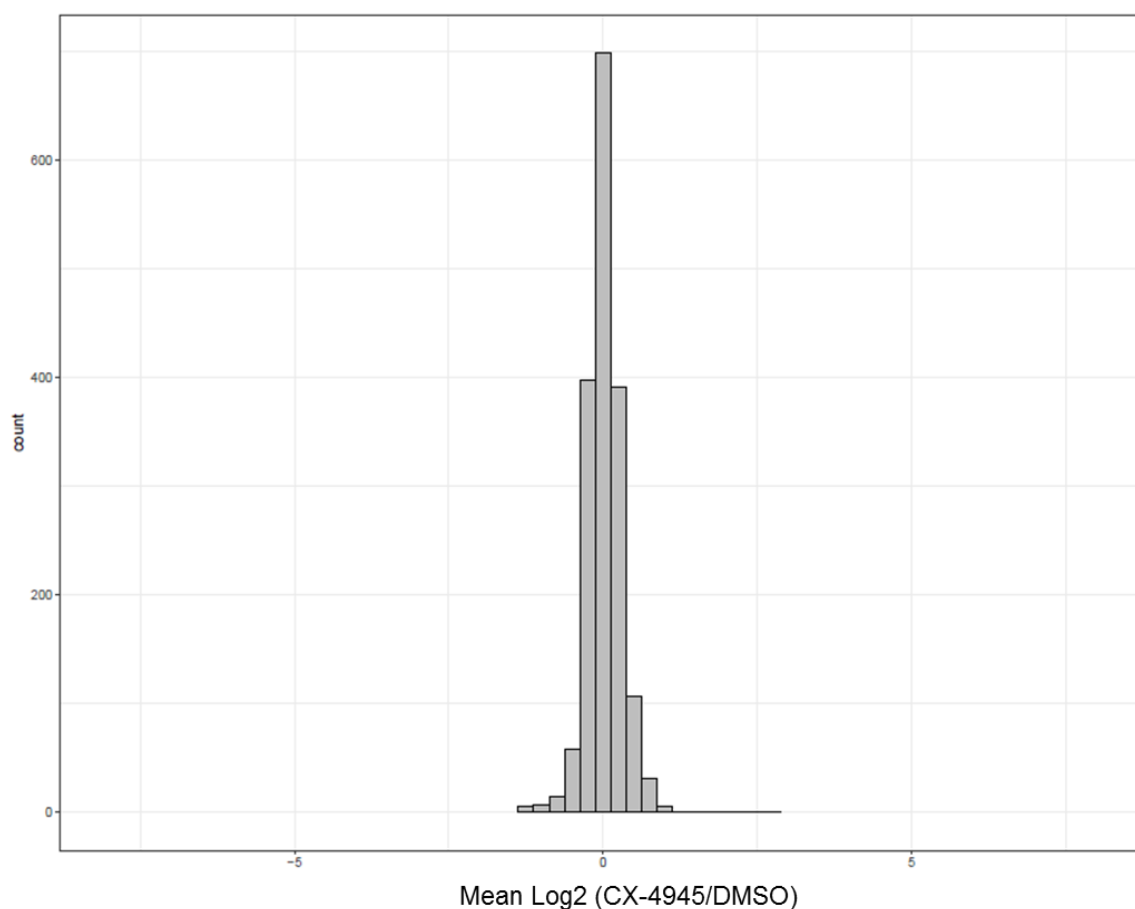
16 (Supplemental Figure 5). Preliminary Time-Course treatment of U2OS cells with 50 μ M CX-4945 and 1 μ M Staurosporine. Parental Flp-U2OS cells were treated for intervals up to 6 hours with CX-4945 and pan-kinase inhibitor Staurosporine. Lysates were collected and separated by SDS-PAGE, transferred and western blotted using antibodies against PARP-1.



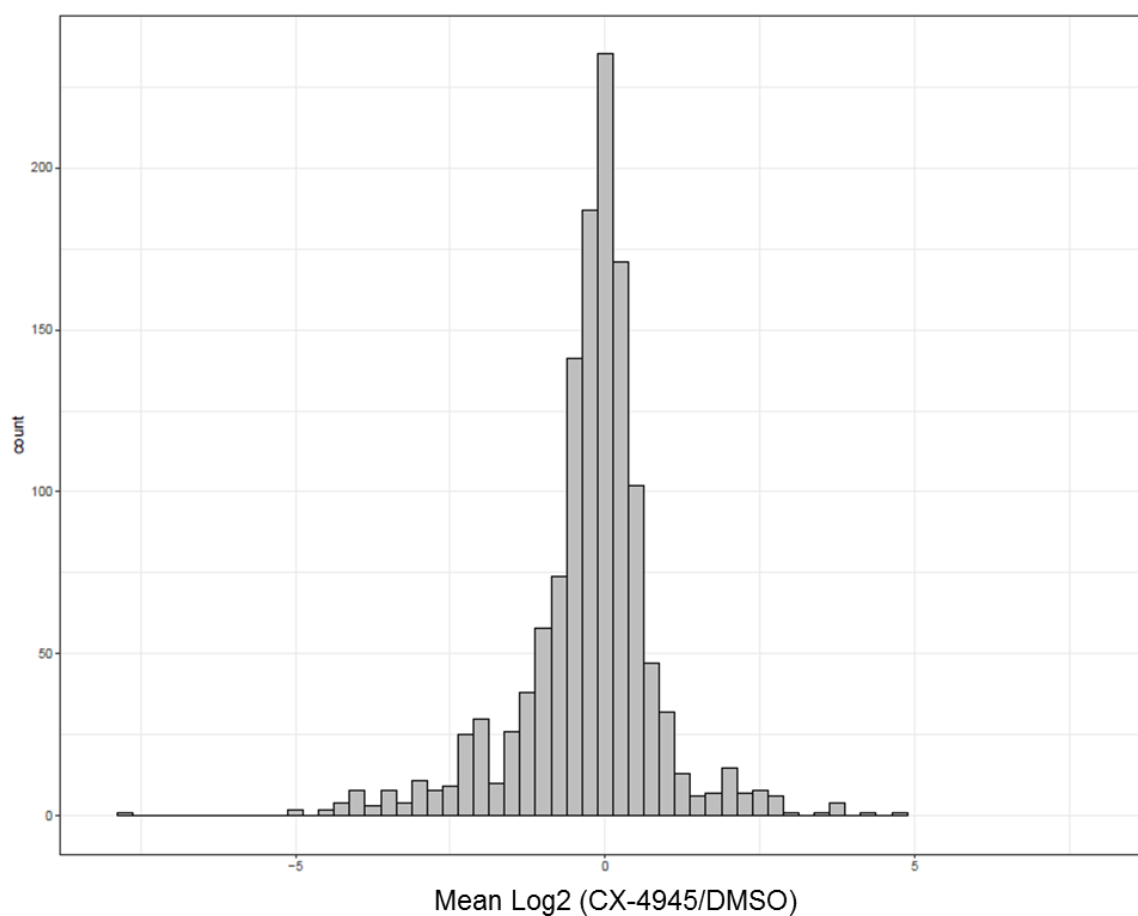
17 (Supplemental Figure 6). Quantified CK2 Phosphorylation Sites in PhosphositePlus in U2OS Cells Treated with 30 μ M CX-4945. Phosphorylation sites listed as CK2 substrates are presented along with their fold change. Fold change represents the mean calculated value from four biological replicates.



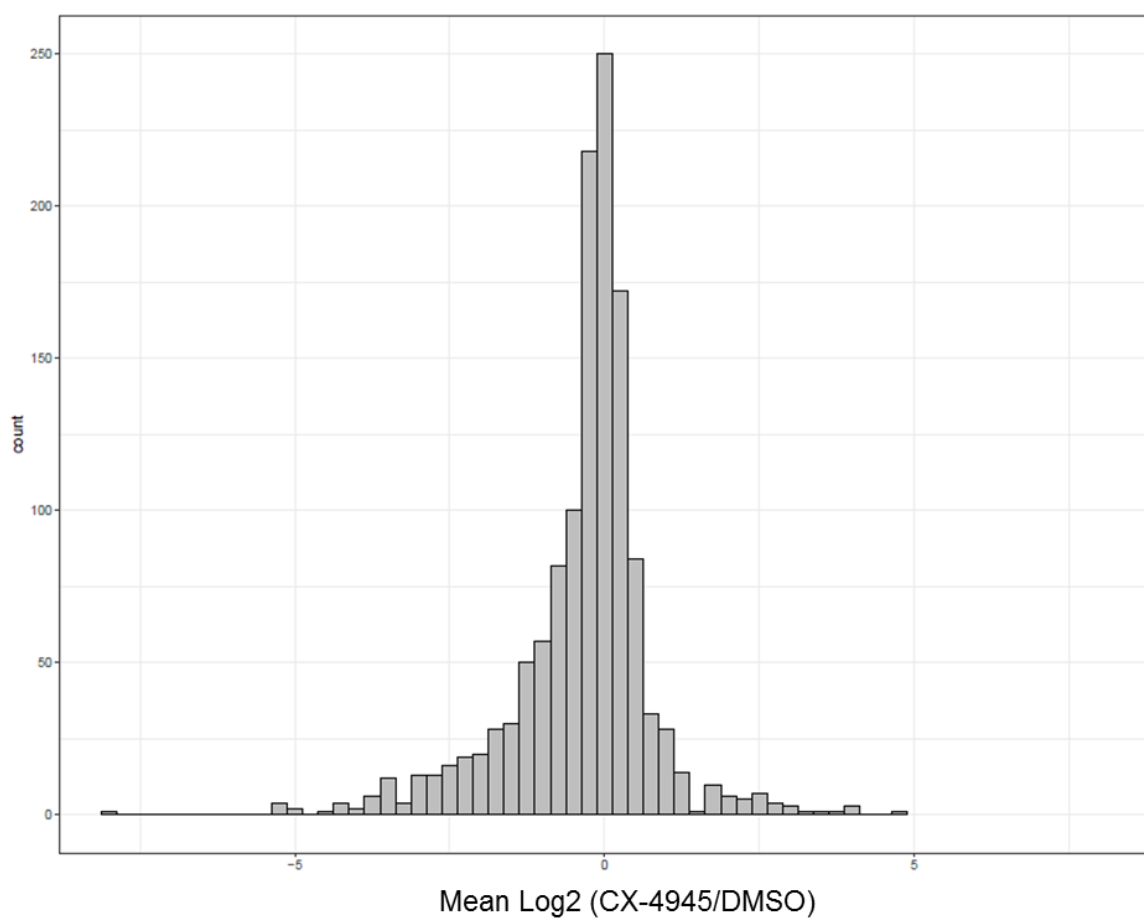
18 (Supplemental figure 7). Frequency Distribution of Protein Mean Log2 Ratio in Flp-U2OS cells expressing wild-type CK2-alpha treated with 30 μ M CX-4945 for 4 hours. The mean log2 ratio of four biological replicates for each protein group identified and quantified is displayed. All quantified proteins from U2OS cells treated with 30 μ M CX-4945 are represented.



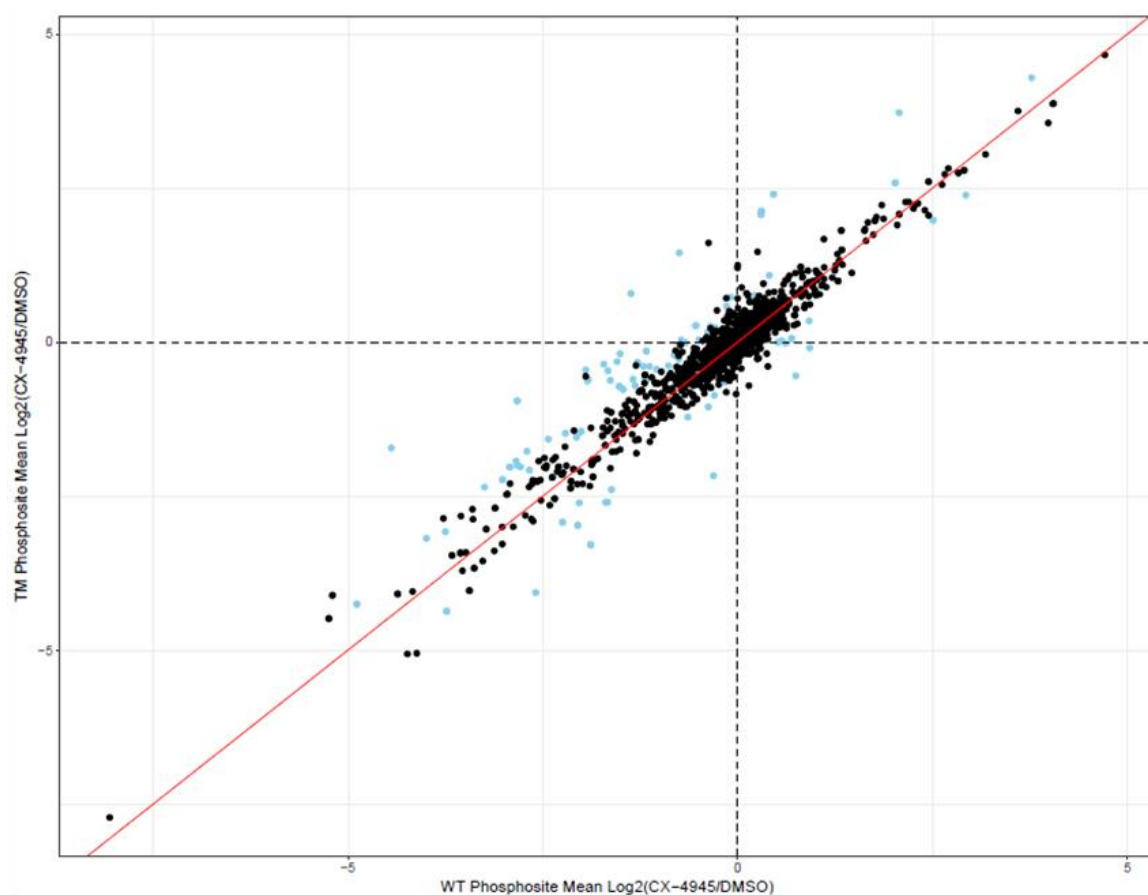
19 (Supplemental Figure 8). Frequency Distribution of Protein Mean Log2 Ratio in Flp-U2OS cells expressing inhibitor-refractory CK2-alpha treated with 30 μ M CX-4945 for 4 hours. The mean log2 ratio of four biological replicates for each protein group identified and quantified is displayed. All quantified proteins from U2OS cells treated with 30 μ M CX-4945 are represented.



20 (Supplemental Figure 9). Frequency Distribution of Phosphorylation Site Mean Log2 Ratio in Flp-U2OS cells expressing inhibitor-refractory CK2-alpha treated with 30 μ M CX-4945 for 4 hours. The mean log2 ratio of four biological replicates for each phosphorylation site identified and quantified is displayed. All quantified proteins from U2OS cells treated with 30 μ M CX-4945 are represented.



21 (Supplementary Figure 10). Frequency Distribution of Phosphorylation Site Mean Log2 Ratio in Flp-U2OS cells expressing With-Type CK2-alpha treated with 30 μ M CX-4945 for 4 hours. The mean log2 ratio of four biological replicates for each phosphorylation site identified and quantified is displayed. All quantified proteins from U2OS cells treated with 30 μ M CX-4945 are represented.



Supplemental Figure 11. Bi-plot of Phosphorylation Site Mean Log2 Fold Changes for U2OS Cells Expressing either Wild-Type or Inhibitor Refractory CK2-alpha Treated with 30 μ M CX-4945. Mean log2 ratios of identified and quantified phosphorylation sites for wild-type and inhibitor-refractory CK2alpha expressing U2OS cell lines were plotted against each other. Correlation was calculated to be 0.94. Red line represents a slope of 1.

Bibliography

1. Graves, J. D., and Krebs, E. G. (1999) Protein Phosphorylation and Signal Transduction. *Pharmacol. Ther.* **82**, 2–3
2. Cohen, P. (2002) Protein kinases — the major drug targets of the twenty-first century? *Nat. Rev. Drug Discov.* **1**, 309–315
3. Manning, G., Whyte, D. B., Martinez, R., Hunter, T., and Sudarsanam, S. (2002) The protein kinase complement of the human genome. *Science*. **298**, 1912–34
4. Brognard, J., Hunter, T., Marshall, C., and Vousden, K. (2010) Protein kinase signaling networks in cancer This review comes from a themed issue on Genetic and cellular mechanisms of oncogenesis Edited. *Curr. Opin. Genet. Dev.* **21**, 4–11
5. Zhang, J., Yang, P. L., and Gray, N. S. (2009) Targeting cancer with small molecule kinase inhibitors. *Nat. Rev. Cancer*. **9**, 28–39
6. Lydon, N. B., and Druker, B. J. (2004) Lessons learned from the development of imatinib. *Leuk. Res.* **28**, 29–38
7. Rask-Andersen, M., Masuram, S., and Schiöth, H. B. (2014) The Druggable Genome: Evaluation of Drug Targets in Clinical Trials Suggests Major Shifts in Molecular Class and Indication. *Annu. Rev. Pharmacol. Toxicol.* **54**, 9–26
8. Olsen, B. B., Guerra, B., Niefind, K., and Issinger, O.-G. (2010) Structural Basis of the Constitutive Activity of Protein Kinase CK2. *Methods in Enzym.* **484**, 515–529.
9. Sarno, S., Ghisellini, P., and Pinna, L. A. (2002) Unique activation mechanism of protein kinase CK2. The N-terminal segment is essential for constitutive activity of the catalytic subunit but not of the holoenzyme. *J. Biol. Chem.* **277**, 22509–14
10. Yang-Feng, T. L., Zheng, K., Kopatz, I., Naiman, T., and Canaanil, D. Mapping of the human casein kinase 11 catalytic subunit genes: two loci carrying the homologous sequences for the α subunit. *Nucleic Acids Res.* **19**, 7125–7129
11. Litchfield, D. W., and Luscher, B. (1993) Casein kinase II in signal transduction and cell cycle regulation. *Mol. Cell. Biochem.* **127–128**, 187–199
12. Poletto, G., Vilardell, J., Marin, O., Pagano, M. A., Cozza, G., Sarno, S., Falqués, A., Itarte, E., Pinna, L. A., and Meggio, F. (2008) The Regulatory β Subunit of Protein Kinase CK2 Contributes to the Recognition of the Substrate Consensus Sequence. A Study with an eIF2 β -Derived Peptide † . *Biochemistry*. **47**, 8317–8325

13. Turowec, J. P., Vilks, G., Gabriel, M., and Litchfield, D. W. (2013) Characterizing the convergence of protein kinase CK2 and caspase-3 reveals isoform-specific phosphorylation of caspase-3 by CK2 α' : implications for pathological roles of CK2 in promoting cancer cell survival. *Oncotarget*. **4**, 560–71
14. Meggio, F., and Pinna, L. A. (2003) One-thousand-and-one substrates of protein kinase CK2? *FASEB J.* **17**, 349–68
15. Salvi, M., Sarno, S., Cesaro, L., Nakamura, H., and Pinna, L. A. (2009) Extraordinary pleiotropy of protein kinase CK2 revealed by weblogo phosphoproteome analysis. *Biochim. Biophys. Acta - Mol. Cell Res.* **1793**, 847–859
16. Homma, M. K., and Homma, Y. (2008) Cell cycle and activation of CK2. *Mol. Cell. Biochem.* **316**, 49–55
17. Ahmed, K., Gerber, D. A., and Cochet, C. (2002) Joining the cell survival squad: an emerging role for protein kinase CK2. *Trends Cell Biol.* **12**, 226–30
18. Tsuchiya, Y., Akashi, M., Matsuda, M., Goto, K., Miyata, Y., Node, K., and Nishida, E. (2009) Involvement of the Protein Kinase CK2 in the Regulation of Mammalian Circadian Rhythms. *Sci. Signal.* [online]
19. Piazza, F. A., Ruzzene, M., Gurrieri, C., Montini, B., Bonanni, L., Chioetto, G., Di Maira, G., Barbon, F., Cabrelle, A., Zambello, R., Adami, F., Trentin, L., Pinna, L. A., and Semenzato, G. (2006) Multiple myeloma cell survival relies on high activity of protein kinase CK2. *Blood*. 108(5), 1698-1707
20. Timmer, J. C., and Salvesen, G. S. (2007) Caspase substrates. *Cell Death Differ.* **14**, 66–72
21. Duncan, J. S., Turowec, J. P., Duncan, K. E., Vilks, G., Wu, C., Lüscher, B., Li, S. S.-C., Gloor, G. B., and Litchfield, D. W. (2011) A Peptide-Based Target Screen Implicates the Protein Kinase CK2 in the Global Regulation of Caspase Signaling. *Sci. Signal.* 4(172), ra30-ra3
22. Gyenis, L., Duncan, J. S., Turowec, J. P., Bretner, M., and Litchfield, D. W. (2011) Unbiased Functional Proteomics Strategy for Protein Kinase Inhibitor Validation and Identification of *bona fide* Protein Kinase Substrates: Application to Identification of EEF1D as a Substrate for CK2. *J. Proteome Res.* **10**, 4887–4901
23. Riman, S., Rizkallah, R., Kassardjian, A., Alexander, K. E., Luscher, B., and Hurt, M. M. (2012) Phosphorylation of the Transcription Factor YY1 by CK2 Prevents Cleavage by Caspase 7 during Apoptosis. *Mol. Cell. Biol.* **32**, 797–807

24. Desagher, S., Osen-Sand, A., Montessuit, S., Magnenat, E., Vilbois, F., Hochmann, A., Journot, L., Antonsson, B., and Martinou, J.-C. (2001) Phosphorylation of Bid by Casein Kinases I and II Regulates Its Cleavage by Caspase 8. *Mol. Cell.* **8**, 601–611
25. Duncan, J. S., Turowec, J. P., Duncan, K. E., Vilk, G., Wu, C., Lüscher, B., Li, S. S.-C., Gloor, G. B., and Litchfield, D. W. A Peptide-Based Target Screen Implicates the Protein Kinase CK2 in the Global Regulation of Caspase Signaling. *Sci. Signal.* 4(172), ra30-ra
26. Turowec, J. P., Zukowski, S. A., Knight, J. D. R., Smalley, D. M., Graves, L. M., Johnson, G. L., Li, S. S. C., Lajoie, G. A., and Litchfield, D. W. An Unbiased Proteomic Screen Reveals Caspase Cleavage Is Positively and Negatively Regulated by Substrate Phosphorylation*. 10.1074/mcp.M113.037374
27. Tawfic, S., Yu, S., Wang, H., Faust, R., Davis, A., and Ahmed, K. (2001) Review Protein kinase CK2 signal in neoplasia. *Histology and histopathology*, 16(2), 573–582
28. Yoo, J.-Y., Lim, B. J., Choi, H.-K., Hong, S. W., Jang, H. S., Kim, C., Chun, K.-H., Choi, K.-C., and Yoon, H.-G. (2013) CK2-NCoR signaling cascade promotes prostate tumorigenesis. *Oncotarget.* **4**, 972–83
29. Yu, M., Yeh, J., and Van Waes, C. (2006) Protein kinase casein kinase 2 mediates inhibitor-kappaB kinase and aberrant nuclear factor-kappaB activation by serum factor(s) in head and neck squamous carcinoma cells. *Cancer Res.* **66**, 6722–31
30. Scaglioni, P. P., Yung, T. M., Cai, L. F., Erdjument-Bromage, H., Kaufman, A. J., Singh, B., Teruya-Feldstein, J., Tempst, P., and Pandolfi, P. P. (2006) A CK2-dependent mechanism for degradation of the PML tumor suppressor. *Cell.* **126**, 269–83
31. Stalter, G., Siemer, S., Becht, E., Ziegler, M., Remberger, K., and Issinger, O. G. (1994) Asymmetric expression of protein kinase CK2 subunits in human kidney tumors. *Biochem. Biophys. Res. Commun.* **202**, 141–7
32. Seldin, D. C., and Leder, P. (1995) Casein kinase II alpha transgene-induced murine lymphoma: relation to theileriosis in cattle. *Science.* **267**, 894–7
33. Romieu-Mourez, R., Landesman-Bollag, E., Seldin, D. C., and Sonenshein, G. E. (2002) Protein kinase CK2 promotes aberrant activation of nuclear factor-kappaB, transformed phenotype, and survival of breast cancer cells. *Cancer Res.* **62**, 6770–8
34. Ruzzene, M., and Pinna, L. A. (2009) Addiction to protein kinase CK2: A common denominator of diverse cancer cells? *BBA - Proteins Proteomics.* **1804**, 499–504

35. Unger, G. M., Davis, A. T., Slaton, J. W., and Ahmed, K. (2004) Protein kinase CK2 as regulator of cell survival: implications for cancer therapy. *Curr. Cancer Drug Targets*. **4**, 77–84
36. Montenarh, M. Protein kinase CK2 and angiogenesis. *Adv. Clin. Exp. Med.* **23**, 153–8
37. Shao, J., Prince, T., Hartson, S. D., and Matts, R. L. (2003) Phosphorylation of Serine 13 Is Required for the Proper Function of the Hsp90 Co-chaperone, Cdc37. *J. Biol. Chem.* **278**, 38117–38120
38. Miyata, Y., and Nishida, E. (2005) CK2 binds, phosphorylates, and regulates its pivotal substrate Cdc37, an Hsp90-cochaperone. *Mol. Cell. Biochem.* **274**, 171–9
39. Di Maira, G., Brustolon, F., Bertacchini, J., Tosoni, K., Marmioli, S., Pinna, L. A., and Ruzzene, M. (2007) Pharmacological inhibition of protein kinase CK2 reverts the multidrug resistance phenotype of a CEM cell line characterized by high CK2 level. *Oncogene*. **26**, 6915–26
40. Ortega, C. E., Seidner, Y., and Dominguez, I. (2014) Mining CK2 in Cancer. *PLoS One*. **9**, e115609
41. Filhol, O., Giacosa, S., Wallez, Y., and Cochet, C. (2015) Protein kinase CK2 in breast cancer: the CK2 β regulatory subunit takes center stage in epithelial plasticity. *Cell. Mol. Life Sci.* **72**, 3305–3322
42. Hung, M.-S., Lin, Y.-C., Mao, J.-H., Kim, I.-J., Xu, Z., Yang, C.-T., Jablons, D. M., and You, L. (2010) Functional polymorphism of the CK2 α intronless gene plays oncogenic roles in lung cancer. *PLoS One*. **5**, e11418
43. Duncan, J. S., and Litchfield, D. W. (2008) Too much of a good thing: the role of protein kinase CK2 in tumorigenesis and prospects for therapeutic inhibition of CK2. *Biochim. Biophys. Acta*. **1784**, 33–47
44. Cozza, G., and Pinna, L. A. (2016) Casein kinases as potential therapeutic targets. *Expert Opin. Ther. Targets*. **20**, 319–340
45. Cozza, G., Pinna, L. A., and Moro, S. (2012) Protein kinase CK2 inhibitors: a patent review. *Expert Opin. Ther. Pat.* **22**, 1081–97
46. Duncan, J. S., Haystead, T. A. J., and Litchfield, D. W. (2012) Chemoproteomic Characterization of Protein Kinase Inhibitors Using Immobilized ATP. in *Methods in molecular biology (Clifton, N.J.)*, pp. 119–134, **795**, 119–134
47. Pierre, F., Chua, P. C., O'Brien, S. E., Siddiqui-Jain, A., Bourbon, P., Haddach, M., Michaux, J., Nagasawa, J., Schwaebe, M. K., Stefan, E., Vialettes, A., Whitten, J. P., Chen, T. K., Darjania, L., Stansfield, R., Anderes, K., Bliesath, J., Drygin, D., Ho, C., Omori, M., Proffitt, C., Streiner, N., Trent, K., Rice, W. G.,

- and Ryckman, D. M. (2011) Discovery and SAR of 5-(3-Chlorophenylamino)benzo[*c*][2,6]naphthyridine-8-carboxylic Acid (CX-4945), the First Clinical Stage Inhibitor of Protein Kinase CK2 for the Treatment of Cancer. *J. Med. Chem.* **54**, 635–654
48. Battistutta, R., Cozza, G., Pierre, F., Papinutto, E., Lolli, G., Sarno, S., O'Brien, S. E., Siddiqui-Jain, A., Haddach, M., Anderes, K., Ryckman, D. M., Meggio, F., and Pinna, L. a (2011) Unprecedented selectivity and structural determinants of a new class of protein kinase CK2 inhibitors in clinical trials for the treatment of cancer. *Biochemistry*. **50**, 8478–88
 49. Sarno, S., Salvi, M., Battistutta, R., Zanotti, G., and Pinna, L. A. (2005) Features and potentials of ATP-site directed CK2 inhibitors. *Biochim. Biophys. Acta*. **1754**, 263–70
 50. Pierre, F., Chua, P. C., O'Brien, S. E., Siddiqui-Jain, A., Bourbon, P., Haddach, M., Michaux, J., Nagasawa, J., Schwaebe, M. K., Stefan, E., Vialettes, A., Whitten, J. P., Chen, T. K., Darjanian, L., Stansfield, R., Bliesath, J., Drygin, D., Ho, C., Omori, M., Proffitt, C., Streiner, N., Rice, W. G., Ryckman, D. M., and Anderes, K. (2011) Pre-clinical characterization of CX-4945, a potent and selective small molecule inhibitor of CK2 for the treatment of cancer. *Mol. Cell. Biochem.* **356**, 37–43
 51. Mazzorana, M., Pinna, L. A., and Battistutta, R. (2008) A structural insight into CK2 inhibition. *Mol. Cell. Biochem.* **316**, 57–62
 52. Haynes, K. A., and Silver, P. A. (2011) Synthetic reversal of epigenetic silencing. *J. Biol. Chem.* **286**, 27176–82
 53. Aebersold, R., and Mann, M. (2016) Mass-spectrometric exploration of proteome structure and function. *Nature*. **537**, 347–355
 54. Thakur, S. S., Geiger, T., Chatterjee, B., Bandilla, P., Fröhlich, F., Cox, J., and Mann, M. (2011) Deep and Highly Sensitive Proteome Coverage by LC-MS/MS Without Prefractionation. *Mol. Cell. Proteomics*. **10**, M110.003699
 55. Hebert, A. S., Richards, A. L., Bailey, D. J., Ulbrich, A., Coughlin, E. E., Westphall, M. S., and Coon, J. J. (2014) The One Hour Yeast Proteome. *Mol. Cell. Proteomics*. **13**, 339–347
 56. Smith, L. M., Kelleher, N. L., Linial, M., Goodlett, D., Langridge-Smith, P., Ah Goo, Y., Safford, G., Bonilla*, L., Kruppa, G., Zubarev, R., Rontree, J., Chamot-Rooke, J., Garavelli, J., Heck, A., Loo, J., Penque, D., Hornshaw, M., Hendrickson, C., Pasa-Tolic, L., Borchers, C., Chan, D., Young*, N., Agar, J., Masselon, C., Gross*, M., McLafferty, F., Tsybin, Y., Ge, Y., Sanders*, I., Langridge, J., Whitelegge*, J., and Marshall, A. (2013) Proteoform: a single term describing protein complexity. *Nat. Methods*. **10**, 186–187

57. Fenn, J., Mann, M., Meng, C., Wong, S., and Whitehouse, C. (1989) Electrospray ionization for mass spectrometry of large biomolecules. *Science*. 246(4926), 64-71.
58. Bantscheff, M., Schirle, M., Sweetman, G., Rick, J., and Kuster, B. (2007) Quantitative mass spectrometry in proteomics: a critical review. *Anal. Bioanal. Chem.* **389**, 1017–1031
59. Ross, P. L., Huang, Y. N., Marchese, J. N., Williamson, B., Parker, K., Hattan, S., Khainovski, N., Pillai, S., Dey, S., Daniels, S., Purkayastha, S., Juhasz, P., Martin, S., Bartlett-Jones, M., He, F., Jacobson, A., and Pappin, D. J. (2004) Multiplexed Protein Quantitation in *Saccharomyces cerevisiae* Using Amine-reactive Isobaric Tagging Reagents. *Mol. Cell. Proteomics*. **3**, 1154–1169
60. Andrew Thompson, †, Jürgen Schäfer, ‡, Karsten Kuhn, ‡, Stefan Kienle, ‡, Josef Schwarz, ‡, Günter Schmidt, †, Thomas Neumann, ‡ and, and Christian Hamon*, ‡ (2003) Tandem Mass Tags: A Novel Quantification Strategy for Comparative Analysis of Complex Protein Mixtures by MS/MS. *Anal. Chem.*, 2003, 75 (8), pp 1895–1904
61. Boersema, P. J., Raijmakers, R., Lemeer, S., Mohammed, S., and Heck, A. J. R. (2009) Multiplex peptide stable isotope dimethyl labeling for quantitative proteomics. *Nature Protocols* 4,484-494
62. Ong, S. E., and Mann, M. (2006) A practical recipe for stable isotope labeling by amino acids in cell culture (SILAC). *Nat Protoc.* **1**, 2650–2660
63. Cox, J., and Mann, M. (2008) MaxQuant enables high peptide identification rates, individualized p.p.b.-range mass accuracies and proteome-wide protein quantification. *Nat. Biotechnol.* **26**, 1367–1372
64. Tyanova, S., Temu, T., and Cox, J. (2016) The MaxQuant computational platform for mass spectrometry-based shotgun proteomics. *Nat. Protoc.* **11**, 2301–2319
65. Cohen, P. (2002) The origins of protein phosphorylation. *Nat. Cell Biol.* **4**, E127–E130
66. Riley, N. M., and Coon, J. J. (2016) Phosphoproteomics in the Age of Rapid and Deep Proteome Profiling. *Anal. Chem.* **88**, 74–94
67. Steen, H., Jebanathirajah, J. A., Rush, J., Morrice, N., and Kirschner, M. W. (2006) Phosphorylation analysis by mass spectrometry: myths, facts, and the consequences for qualitative and quantitative measurements. *Mol. Cell. Proteomics*. **5**, 172–81
68. Leitner, A. (2010) Phosphopeptide enrichment using metal oxide affinity chromatography. *TrAC Trends Anal. Chem.* **29**, 177–185

69. Sun, Z., Hamilton, K. L., and Reardon, K. F. Evaluation of Quantitative Performance of Sequential Immobilized Metal Affinity Chromatographic Enrichment for Phosphopeptides. *Anal Biochem*, **445**, pp.30-37
70. Carrascal, M., Ovelleiro, D., Casas, V., Gay, M., and Abian, J. (2008) Phosphorylation Analysis of Primary Human T Lymphocytes Using Sequential IMAC and Titanium Oxide Enrichment. *J. Proteome Res.* **7**, 5167–5176
71. Larsen, M. R., Thingholm, T. E., Jensen, O. N., Roepstorff, P., and Jørgensen, T. J. D. (2005) Highly selective enrichment of phosphorylated peptides from peptide mixtures using titanium dioxide microcolumns. *Mol. Cell. Proteomics.* **4**, 873–86
72. Parker, R., Clifton-Bligh, R., and Molloy, M. P. (2014) Phosphoproteomics of MAPK Inhibition in BRAF-Mutated Cells and a Role for the Lethal Synergism of Dual BRAF and CK2 Inhibition. *Mol. Cancer Ther.* (13) (7) 1894-1906
73. Scutt, P. J., Chu, M. L. H., Sloane, D. A., Cherry, M., Bignell, C. R., Williams, D. H., and Evers, P. A. (2009) Discovery and Exploitation of Inhibitor-resistant Aurora and Polo Kinase Mutants for the Analysis of Mitotic Networks. *The Journal of biological chemistry.* vol: 284 (23) pp: 15880-93
74. Horn, H., Schoof, E. M., Kim, J., Robin, X., Miller, M. L., Diella, F., Palma, A., Cesareni, G., Jensen, L. J., and Linding, R. (2014) KinomeXplorer: an integrated platform for kinome biology studies. *Nat. Methods.* **11**, 603–604
75. Yang, P., Patrick, E., Humphrey, S. J., Ghazanfar, S., James, D. E., Jothi, R., and Yang, J. Y. H. (2016) KinasePA: Phosphoproteomics data annotation using hypothesis driven kinase perturbation analysis. *Proteomics.* **16**, 1868–1871
76. Weidner, C., Fischer, C., and Sauer, S. (2014) PHOXTRACK - a tool for interpreting comprehensive data sets of posttranslational modifications of proteins. *Bioinformatics.* **30**, 3410–3411
77. Hornbeck, P. V., Kornhauser, J. M., Tkachev, S., Zhang, B., Skrzypek, E., Murray, B., Latham, V., and Sullivan, M. (2012) PhosphoSitePlus: a comprehensive resource for investigating the structure and function of experimentally determined post-translational modifications in man and mouse. *Nucleic Acids Res.* **40**, D261–D270
78. Mi, H., Muruganujan, A., and Thomas, P. D. PANTHER in 2013: modeling the evolution of gene function, and other gene attributes, in the context of phylogenetic trees. *Nucleic Acids Res*, 41(D1), pp.D377-D386.
79. Chou, M. F., and Schwartz, D. (2011) Biological Sequence Motif Discovery Using *motif-x*. in *Current Protocols in Bioinformatics*, p. Unit 13.15-24, John Wiley & Sons, Inc., Hoboken, NJ, USA, **Chapter 13**, Unit 13.15-24
80. Schwartz, D., and Gygi, S. P. (2005) An iterative statistical approach to the

- identification of protein phosphorylation motifs from large-scale data sets. *Nat. Biotechnol.* **23**, 1391–1398
81. Guerra, B., and Issinger, O.-G. (1999) Protein kinase CK2 and its role in cellular proliferation, development and pathology. *Electrophoresis.* **20**, 391–408
 82. Vilks, G., Derksen, D. R., and Litchfield, D. W. (2001) Inducible expression of the regulatory protein kinase CK2 β subunit: incorporation into complexes with catalytic CK2 subunits and re-examination of the effects of CK2 β on cell proliferation. *J. Cell. Biochem.* **84**, 84–99
 83. Pagano, M. A., Sarno, S., Poletto, G., Cozza, G., Pinna, L. A., and Meggio, F. (2005) Autophosphorylation at the regulatory β subunit reflects the supramolecular organization of protein kinase CK2. *Mol. Cell. Biochem.* **274**, 23–29
 84. Bendall, S. C., Hughes, C., Stewart, M. H., Doble, B., Bhatia, M., and Lajoie, G. a (2008) Prevention of amino acid conversion in SILAC experiments with embryonic stem cells. *Mol. Cell. Proteomics.* **7**, 1587–97
 85. Rabalski, A. J. (2017) Quantitative Proteomic Characterization of CX-4945, a Clinical Stage Inhibitor of Protein Kinase CK2
 86. Litchfield, D. W. (2003) Protein kinase CK2: structure, regulation and role in cellular decisions of life and death. *Biochem. J.*, 369(1), pp.1-15
 87. Wu, R., Haas, W., Dephoure, N., Huttlin, E. L., Zhai, B., Sowa, M. E., and Gygi, S. P. A large-scale method to measure absolute protein phosphorylation stoichiometries. *Nat Meth* , 8(8), 677-683.
 88. Jiang, X., Feng, S., Chen, Y., Feng, Y., & Deng, H. (2016). Proteomic analysis of mTOR inhibition- mediated phosphorylation changes in ribosomal proteins and eukaryotic translation initiation factors. *Protein Cell.* 533-537.
 89. Lee, J. H., Pestova, T. V, Shin, B.-S., Cao, C., Choi, S. K., and Dever, T. E. (2002) Initiation factor eIF5B catalyzes second GTP-dependent step in eukaryotic translation initiation. *Proc. Natl. Acad. Sci. U. S. A.* **99**, 16689–94
 90. Gandin, V., Masvidal, L., Cargnello, M., Gyenis, L., McLaughlan, S., Cai, Y., Tenkerian, C., Morita, M., Balanathan, P., Jean-Jean, O., Stambolic, V., Trost, M., Furic, L., Larose, L., Koromilas, A. E., Asano, K., Litchfield, D., Larsson, O., and Topisirovic, I. (2016) mTORC1 and CK2 coordinate ternary and eIF4F complex assembly. *Nat. Commun* , 7, 11127.
 91. Grifo, J. A., Tahara, S. M., Morgan, M. A., Shatkin, A. J., and Merrick, W. C. (1983) New initiation factor activity required for globin mRNA translation. *J. Biol. Chem.* **258**, 5804–10
 92. Wells, N. J., Addison, C. M., Fry, A. M., Ganapathi, R., and Hickson, I. D. (1994)

Serine 1524 is a major site of phosphorylation on human topoisomerase II alpha protein *in vivo* and is a substrate for casein kinase II *in vitro*. *J. Biol. Chem.* **269**, 29746–51

93. Tang, J., Zhang, Z.-H., Huang, M., Heise, T., Zhang, J., and Liu, G.-L. (2013) Phosphorylation of human La protein at Ser³⁶⁶ by casein kinase II contributes to hepatitis B virus replication and expression *in vitro*. *J. Viral Hepat.* **20**, 24–33
94. Franchin, C., Cesaro, L., Salvi, M., Million, R., Iori, E., Cifani, P., James, P., Arrigoni, G., and Pinna, L. (2015) Quantitative analysis of a phosphoproteome readily altered by the protein kinase CK2 inhibitor quinalizarin in HEK-293T cells. *Biochim. Biophys. Acta - Proteins Proteomics.* **1854**, 609–623
95. St-Denis, N., Gabriel, M., Turowec, J. P., Gloor, G. B., Li, S. S.-C., Gingras, A.-C., and Litchfield, D. W. (2015) Systematic investigation of hierarchical phosphorylation by protein kinase CK2. *J. Proteomics.* **118**, 49–62
96. Wang, L., Lawrence, J. C., Sturgill, T. W., and Harris, T. E. (2009) Mammalian Target of Rapamycin Complex 1 (mTORC1) Activity Is Associated with Phosphorylation of Raptor by mTOR. *Jour Biol Chem*, 284(22), 14693-14697.
97. Shor, B., Wu, J., Shakey, Q., Toral-Barza, L., Shi, C., Follettie, M., and Yu, K. (2010) Requirement of the mTOR Kinase for the Regulation of Maf1 Phosphorylation and Control of RNA Polymerase III-dependent Transcription in Cancer Cells. *J. Biol. Chem.* **285**, 15380–15392
98. Kim, J., Park, M., Ryu, B. J., and Kim, S. H. (2014) The Protein Kinase 2 Inhibitor CX-4945 Induces Autophagy in Human Cancer Cell Lines. *Bull. Korean Chem. Soc.* **35**, 2985–2989
99. Siddiqui-Jain, A., Drygin, D., Streiner, N., Chua, P., Pierre, F., O'Brien, S. E., Bliesath, J., Omori, M., Huser, N., Ho, C., Proffitt, C., Schwaebe, M. K., Ryckman, D. M., Rice, W. G., and Anderes, K. (2010) CX-4945, an orally bioavailable selective inhibitor of protein kinase CK2, inhibits prosurvival and angiogenic signaling and exhibits antitumor efficacy. *Cancer Res.* **70**, 10288–98
100. Schneider, E., Kartarius, S., Schuster, N., and Montenarh, M. (2002) The cyclin H/cdk7/Mat1 kinase activity is regulated by CK2 phosphorylation of cyclin H. *Oncogene.* **21**, 5031–5037
101. Harper, J. W., and Elledge, S. J. (1998) The role of Cdk7 in CAK function, a retro-retrospective. *Genes Dev.* **12**, 285–9
102. Zhang, W., Liu, H. T., and Tu LIU, H. (2002) MAPK signal pathways in the regulation of cell proliferation in mammalian cells. *Cell Res.* **12**, 9–18

103. Plotnikov, A., Chuderland, D., Karamansha, Y., Livnah, O., and Seger, R. (2011) Nuclear extracellular signal-regulated kinase 1 and 2 translocation is mediated by casein kinase 2 and accelerated by autophosphorylation. *Mol. Cell. Biol.* **31**, 3515–30
104. Schneider, C. C., Götz, C., Hessenauer, A., Günther, J., Kartarius, S., and Montenarh, M. (2011) Down-regulation of CK2 activity results in a decrease in the level of cdc25C phosphatase in different prostate cancer cell lines. *Mol. Cell. Biochem.* **356**, 177–184
105. Hou, Z., Nakanishi, I., Kinoshita, T., Takei, Y., Yasue, M., Misu, R., Suzuki, Y., Nakamura, S., Kure, T., Ohno, H. and Murata, K., 2012. Structure-based design of novel potent protein kinase CK2 (CK2) inhibitors with phenyl-azole scaffolds. *Journal of medicinal chemistry*, 55(6), pp.2899-2903.

Curriculum Vitae

Name: Edward Cruise

Post-secondary University of Western Ontario

Education and London, Ontario, Canada

Degrees: 2011-2015 BMSc

The University of Western Ontario

London, Ontario, Canada

2015-2017 MSc

Honours and Western Scholarship of Distinction 2011

Awards: Dean's honor list 2012-2015

Related Work Teaching Assistant

Experience The University of Western Ontario

2015-2017

Publications: